Article

Cell Reports

Meta-regulation of *Arabidopsis* Auxin Responses Depends on tRNA Maturation

Graphical Abstract

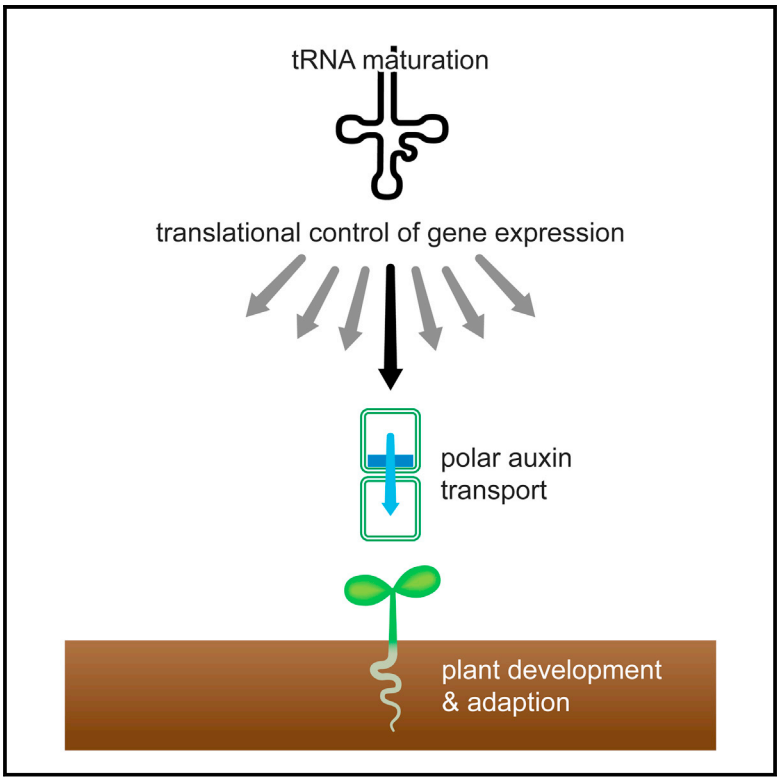

Highlights

- *Arabidopsis* Elongator post-transcriptionally modulates PIN protein levels
- *Arabidopsis* tRNA splicing modulates auxin responses
- *Arabidopsis* tRNA maturation links basic cellular activities to developmental readouts

Authors

Johannes Leitner, Katarzyna Retzer, ..., Anders Byström, Christian Luschnig

Correspondence

christian.luschnig@boku.ac.at

In Brief

Leitner et al. analyze *Arabidopsis* lines deficient in distinct aspects of tRNA maturation, finding defects in control of auxin transport and signaling events. The occurrence of such auxin-related defects as a result of general deficiencies in translational control underlines a rate-limiting function for auxin in plant development.

Leitner et al., 2015, Cell Reports *11*, 516–526
April 28, 2015
http://dx.doi.org/10.1016/j.celrep.2015.03.054

CellPress

OPEN ACCESS
CellPress

Cell Reports
Article

Meta-regulation of *Arabidopsis* Auxin Responses Depends on tRNA Maturation

Johannes Leitner,[1,3] Katarzyna Retzer,[1,3] Nenad Malenica,[1,4] Rasa Bartkeviciute,[1] Doris Lucyshyn,[1] Gunilla Jäger,[2] Barbara Korbei,[1] Anders Byström,[2] and Christian Luschnig[1,*]

[1]Department of Applied Genetics and Cell Biology, University of Natural Resources and Life Sciences, Vienna (BOKU), Muthgasse 18, 1190 Wien, Austria

[2]Department of Molecular Biology, Umeå University, 901 87 Umeå, Sweden

[3]Co-first author

[4]Present address: Department of Molecular Biology, Faculty of Science, University of Zagreb, Horvatovac 102a, 10000 Zagreb, Croatia

*Correspondence: christian.luschnig@boku.ac.at

http://dx.doi.org/10.1016/j.celrep.2015.03.054

SUMMARY

Polar transport of the phytohormone auxin throughout plants shapes morphogenesis and is subject to stringent and specific control. Here, we identify basic cellular activities connected to translational control of gene expression as sufficient to specify auxin-mediated development. Mutants in subunits of *Arabidopsis* Elongator, a protein complex modulating translational efficiency via maturation of tRNAs, exhibit defects in auxin-controlled developmental processes, associated with reduced abundance of PIN-formed (PIN) auxin transport proteins. Similar anomalies are observed upon interference with tRNA splicing by downregulation of *RNA ligase* (*AtRNL*), pointing to a general role of tRNA maturation in auxin signaling. *Elongator Protein 6 (ELP6)* and *AtRNL* expression patterns underline an involvement in adjusting PIN protein levels, whereas rescue of mutant defects by auxin indicates rate-limiting activities in auxin-controlled organogenesis. This emphasizes mechanisms in which auxin serves as a bottleneck for plant morphogenesis, translating common cellular activities into defined developmental readouts.

INTRODUCTION

Sessile plants evolved sophisticated mechanisms to respond to environmental stimuli and developmental cues. Key to several of these processes is the transmission of signals generated by the plant hormone auxin (indole-3-acetic acid, IAA, the predominant form found in plants). Auxin is special among plant hormones as its spectrum of activities requires its active, directional transport throughout the plant body (Peer et al., 2011; Voß et al., 2014; Wabnik et al., 2011). Such polar auxin transport (PAT), together with metabolic control of auxin, defines local variations in hormone levels, which are perceived and transmitted to induce hormonally controlled adjustments in gene expression and activity (Ljung, 2013; Sauer et al., 2013).

Perception of variations in auxin homeostasis and downstream signaling events has been analyzed extensively in the model plant *Arabidopsis*, which led to establishment of pathways specifically required for the transmission of hormonal signals (Boer et al., 2014; Dharmasiri et al., 2005; Kepinski and Leyser, 2005; Paciorek et al., 2005; Ulmasov et al., 1999; Xu et al., 2010). This involves cellular auxin uptake and efflux proteins with plasma membrane-localized PIN proteins implicated in auxin efflux (Petrásek et al., 2006). Here, we describe components of two distinct *Arabidopsis* pathways involved in tRNA maturation and characterize their function in auxin distribution and responses. We show that adjustments in PIN auxin transport protein levels are mediated by a plant ortholog of the multifunctional Elongator complex. In eukaryotes, Elongator has been linked to diverse cellular events, including transcriptional elongation, acetylation of chromatin and cytoskeleton components, protein sorting, as well as post-transcriptional modification of tRNAs (Chen et al., 2009; Esberg et al., 2006; Otero et al., 1999; Rahl et al., 2005; Wittschieben et al., 1999). We provide evidence that alterations in Elongator-mediated tRNA maturation in plants give rise to auxin-related growth deficiencies and PIN mis-expression. In addition, *Arabidopsis* deficient in *AtRNL*, an RNA-ligase required for splicing of tRNAs that do not represent bona fide ELP substrates, exhibits growth defects resembling those of *elp* mutants. This suggests a more common requirement of tRNA maturation for morphogenesis and auxin responses. Expression patterns of *ELP6* and *AtRNL*, together with auxin-induced rescue of growth defects associated with diminished tRNA levels, are consistent with scenarios in which tRNA availability modulates auxin responses.

Overall, we demonstrate that deficiencies in *Arabidopsis* tRNA maturation and availability broadly concern transmission of auxin signals. This underlines rate-limiting roles of the growth regulator in plant morphogenesis and hints at meta-regulatory levels of growth control, by which adjustments in general cellular activities could feed back on defined aspects of plant development via modulation of auxin responses.

RESULTS

Mop Mutants Are Affected in Subunits of an *Arabidopsis* Elongator Complex

In earlier work, we described two *Arabidopsis* mutants termed *mop2-1* and *mop3-1* (for *modulator of PIN*), which both exhibit developmental and patterning defects reminiscent of mutants deficient in PAT (Malenica et al., 2007). This is indicated by altered expression of an auxin-responsive reporter protein and by reduced abundance of PIN auxin transport proteins. Notably, although PIN protein levels are reduced in both *mop* mutants, no corresponding changes in *PIN* transcript levels could be detected, suggesting involvement of both *MOP* loci in post-transcriptional regulation of PINs (Malenica et al., 2007).

Both *mop* mutants are derived from a pool of T-DNA insertion lines (Sieberer et al., 2003). For cloning of *MOP2*, we analyzed F2 populations of *mop2-1*, outcrossed into Col-0 wild-type, and identified a segregating T-DNA insertion in the second intron of locus At4g10090. This locus represents an *Arabidopsis* ortholog of *Elongator protein 6* (*ELP6*), a subunit of Elongator holoenzyme found in eukaryotes from baker's yeast to human (Hawkes et al., 2002; Nelissen et al., 2005; Otero et al., 1999). To test whether *mop2-1* mutant phenotypes could result from this T-DNA insertion we analyzed gene expression, demonstrating a loss of *ELP6* transcription in *mop2-1* (Figure S1B). Transformation of *mop2-1* with a VENUS-tagged ELP6 fusion protein expressed by its endogenous promoter (*ELP6p::VENUS:ELP6*) rescued growth deficiencies, indicating that *mop2-1* defects result from a loss of *ELP6* (Figures S1C and S1D). We therefore termed the former *mop2-1* allele *elp6*^{mop2}.

The Elongator complex was suggested to be composed of 12 subunits, with two copies of each ELP1, 2, and 3 forming a core sub-complex, and an additional accessory sub-complex, composed of two copies of ELP4, 5, and 6 (Glatt and Müller, 2013; Winkler et al., 2001). Given the resemblance of *elp6*^{mop2} and *mop3-1* phenotypes, we reasoned that the latter could be affected in another *ELP* locus and initiated complementation tests between *mop3-1* and T-DNA insertion lines affected in the remaining subunits of *Arabidopsis* Elongator. No complementation of mutant phenotypes was observed in F1 and F2 progeny derived from crosses between *mop3-1* and GK_555H06, deficient in *ELP3* (At5g50320; *ELONGATA 3*, *HISTONE ACETYLTRANSFERASE OF THE GNAT FAMILY 3*). Determination of *ELP3* expression in *mop3-1* demonstrated a loss of full-length transcript (Figure S1B); however, when analyzing the genomic *ELP3* locus in *mop3-1*, we could not characterize a T-DNA insertion but found evidence for rearrangements at this chromosomal position (Leitner, 2011). Therefore, and to minimize potential effects unrelated to defects in *ELP3*, all further experiments were performed with line GK_555H06, harboring a characterized T-DNA insertion in the *ELP3* locus (*elp3*; Xu et al., 2012; Figure S1B).

Arabidopsis Elongator Is Involved in Post-transcriptional Control of PIN Protein Levels

The phenotypic resemblance of *elp6*^{mop2}, *mop3-1*, and *elp3*, suggests that corresponding gene products function as essential subunits of a protein complex, similar to Elongator in other eukaryotes (Glatt and Müller, 2013). We therefore tested mutants defective in the remaining ELP subunits for growth defects (Figure S1B). Homozygous insertion lines for *ELP1/ELO2/ABO1* (At5g13680; SALK_005153), *ELP2* (At1g49540; SALK_106485), *ELP4/ELO1* (At3g11220; SALK_079193), and *ELP5* (At2g18410; GK_700A12) were grown along *elp3* and *elp6*^{mop2}. All these mutants exhibited related defects in shoot and root morphology, manifested at the seedling stage as reduced root elongation and deficiencies in directional root growth along the gravity vector, similar to *mop* alleles (Figures 1A–1C; Malenica et al., 2007). Related developmental defects were observed during later stages of development, affecting leaf and inflorescence morphogenesis (Figure S1A).

Elp phenotypes in patterning and growth responses are reminiscent of mutants in auxin transport and/or signaling (Malenica et al., 2007). In accordance, a comparison of endogenous PIN1 and PIN2 protein levels in all six *elp* mutants demonstrated reduced abundance of these key regulators of auxin transport, and consistent results were obtained when analyzing expression of the *PIN1p::PIN1:GFP* translational reporter gene (Figures 1D and 1E). Defects in protein abundance are not restricted to PINs though, exemplified by reduced accumulation of a BOR1:GFP translational fusion, when overexpressed by the 35S promoter in *elp6*^{mop2} (Figure S2C; Takano et al., 2005).

We analyzed subcellular distribution of PIN1 in further detail and tested for endogenous PIN1 in soluble *elp* protein fractions and determined PIN1:GFP localization at higher resolution. No striking differences to wild-type could be observed in these experiments, suggesting that reduced PIN abundance in the membrane fraction is not an immediate consequence of protein mis-localization (Figures S2A and S2B). Evidence for *elp* deficiencies affecting post-transcriptional regulation of PINs came from analysis of *PIN* transcript levels in the *elp* mutants. Specifically, no decrease in *PIN1* transcript levels was detectable with qPCR, whereas protein levels were decreased (Figure 1D). A slight decrease in transcript levels was observed for *PIN2* in *elp* mutants, which, however, was significant only for *elp2* (Figure 1D).

To test for crosstalk between Elongator and PINs, we generated *PIN1* overexpression constructs under control of the *RP40* ribosomal protein promoter, highly active in meristematic zones (Butt et al., 2014). We made use of this promoter, because attempts to obtain efficient *PIN* overexpression lines in *mop* mutants failed, when using the CaMV 35S promoter (Malenica et al., 2007). Expression of *RP40p::PIN1* in *elp6*^{mop2} resulted in markedly higher PIN1 protein levels, demonstrating that *RP40p*-driven *PIN* expression is well suited for this approach (Figure S3A). When analyzing phenotypes, we found that *elp6*^{mop2} *RP40p::PIN1* primary roots are longer than *elp6*^{mop2} roots of identical age whereas no pronounced difference was observed when comparing wild-type and *RP40p:PIN1*, indicating that reduced abundance of PIN1 contributes to *elp6*^{mop2} root growth defects (Figure 2A). We then determined responses of *elp6*^{mop2} *RP40p::PIN1* to auxin transport inhibitor NPA (1-N-Naphthylphthalamic acid), as *elp6*^{mop2} seedlings are overly sensitive to the compound, reflected in reduced root elongation and defects in root meristem patterning (Figures 2A–2C; Malenica et al., 2007). NPA sensitivity is dampened in *elp6*^{mop2} *RP40p::PIN1*, suggestive of a PIN1 dosage-dependent reversion of NPA

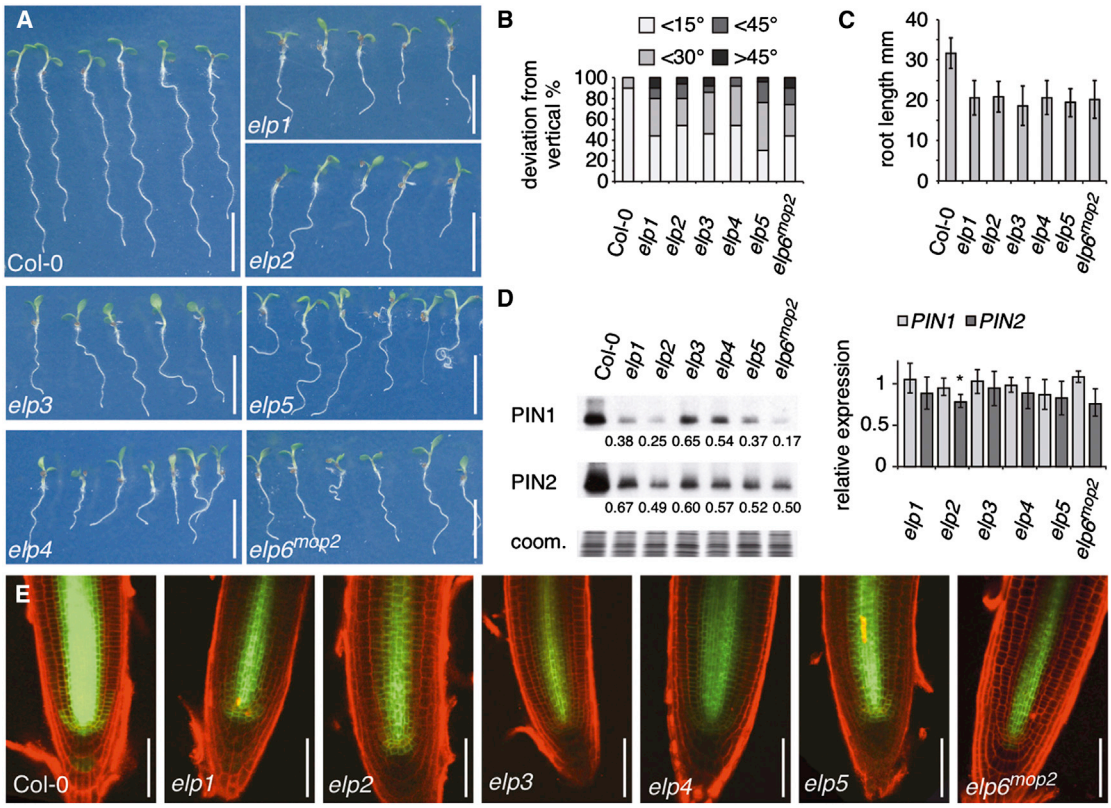

Figure 1. Loss of Elongator Complex in *Arabidopsis* Interferes with Auxin-Controlled Morphogenesis and Post-transcriptional Regulation of PINs

(A) Comparison of wild-type Col-0 and *elp* mutant seedlings at 7 DAG.

(B) Orientation of primary root growth of Col-0 and *elp* seedlings at 9 DAG. A total of 50 seedlings were analyzed for each genotype and plotted as percentage of seedlings displaying <15°, <30°, <45°, and >45° deviation from the vertical growth axes.

(C) Comparison of primary root length of Col-0 and *elp* seedlings at 5 DAG. 20 seedlings were analyzed for each genotype. SDs are indicated.

(D) Quantification of *PIN1* and *PIN2* protein (left panels) and mRNA (right panels) in Col-0 and *elp* seedlings at 7 DAG. Relative signal intensities are indicated below (Col-0 = 1); "coom." displays Coomassie staining of samples used. qPCR performed with Col-0 (= 1) and *elp* mutants displaying transcript levels of *PIN1* and *PIN2*. SDs from three biological repeats with three technical replicates are indicated (*Student's two-tailed t test; $p < 0.05$).

(E) Comparison of *PIN1::PIN1:GFP* signals (green) in Col-0 and *elp* mutant root meristems at 5 DAG. Propidium iodide staining (PI, red) was used for visualizing cell boundaries.

Size bars in represent 10 mm (A) and 50 μm (E). See also Figures S1 and S2.

effects on root elongation (Figure 2A). Consistent with this scenario, NPA-induced ectopic cell proliferation of *elp6*^{mop2} root tips is antagonized by *PIN1* overexpression, illustrated by reduced ectopic formation of root cap cells (Figures 2B and 2C). However, at the stage of flowering, *elp6*^{mop2} *RP40p::PIN1* still exhibits marked morphological defects (Figures S3B and S3C). Thus, while *PIN1* overexpression is not adequate for a full reversion of *elp6*^{mop2} phenotypes, our observations establish a causal link between downregulation of PIN1 and *elp6*^{mop2} root growth defects.

ELP-Mediated tRNA Maturation Influences Auxin Responses in *Arabidopsis*

Arabidopsis Elongator has been associated with diverse processes, revealing widespread roles for the protein complex (Nelissen et al., 2005; Wang et al., 2013b; Xu et al., 2012; Zhou et al., 2009), and phenotypes of the *elp* mutants point toward a distinctive role in transmitting auxin signals, which earlier has been linked to control of transcriptional elongation (Nelissen et al., 2010). In addition, and analogous to Elongator in yeast, a mutation in *Arabidopsis ELP3* was found to be defective in uridine modification of tRNAs, essential for wobble codon recognition during protein translation (Mehlgarten et al., 2010). We analyzed tRNA preparations from *elp6*^{mop2} and *elp3* and observed a reduction in the occurrence of 5-methoxycarbonyl-methyl-2-thiouridine (mcm^5s^2U) and of 5-carbamoyl-methyluridine (ncm^5U) in both mutant alleles (Figure 2D). This is in accordance with earlier observations and substantiates a role of *Arabidopsis* Elongator in tRNA maturation at wobble position 34, to improve wobbling accuracy and translational fidelity (Johansson et al., 2008; Mehlgarten et al., 2010).

Given that Elongator has been linked to several cellular activities, we asked whether explicitly deficiencies in tRNA maturation could contribute to Elongator mutant phenotypes in

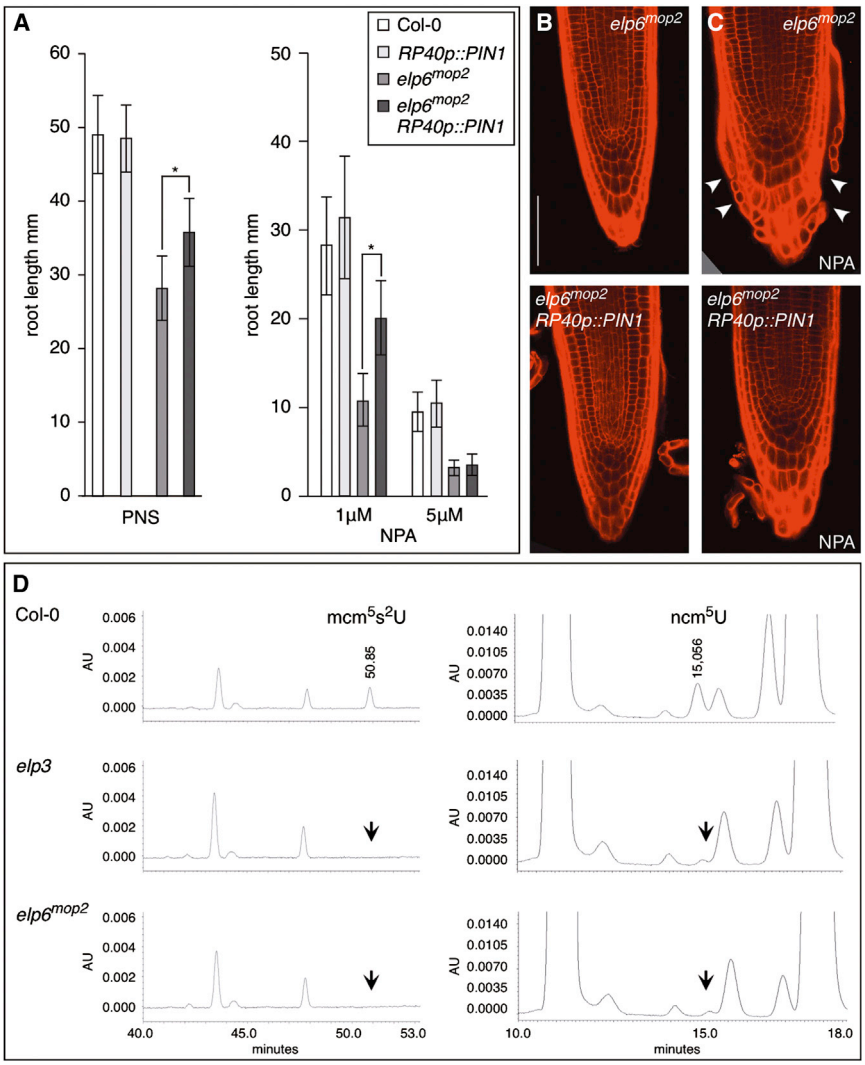

Figure 2. *Elp/mop* Alleles Are Partially Rescued by *PIN1* Overexpression and Characterized by Defects in Ribonucleotide Modifications

(A) Primary root length of Col-0, *elp6*^{mop2}, *RP40p::PIN1* and isogenic *elp6*^{mop2} *RP40p::PIN1* seedlings at 7 DAG, grown on PNS (left) or PNS supplemented with NPA (right). 30–40 seedlings were analyzed for each genotype/condition. SDs are indicated (*Student's two-tailed t test; $p < 0.001$).

(B and C) Comparison of *elp6*^{mop2} and *elp6*^{mop2} *RP40p::PIN1* primary root meristems at 14 DAG grown on PNS (B) or on PNS supplemented with 1 μM NPA (C). White arrowheads indicate increased cell proliferation of *elp6*^{mop2} in response to the auxin transport inhibitor.

(D) Total tRNA fractions isolated from Col-0, *elp3*, and *elp6*^{mop2} were analyzed by HPLC. Left: parts of chromatograms between retention times 40.0 and 53.0 min are displayed. Arrow indicates the expected retention time of mcm^5s^2U. Right: parts of chromatograms between retention times 10.0 and 18.0 min: Arrow indicates the expected retention time of ncm^5U. Chromatograms were monitored at 314 and 254 nm, respectively.

Size bars represent 50 μm (B and C). See also Figure S3.

Arabidopsis. To this end, we made use of *Kluyveromyces lactis* γ-toxin, an endonuclease preferentially degrading tRNAs that underwent modification by Elongator (Lu et al., 2005). Assuming that reduced abundance of Elongator-modified tRNAs contributes to *elp* mutant phenotypes, γ-toxin-mediated degradation of such tRNAs would be expected to give rise to related growth defects. Expression of γ-toxin (*gam*) under control of the *RP40* promoter (Figure 3A) resulted in auxin-related defects, resembling those of *elp* mutants (13/20 lines analyzed). This involved defects in root growth, cotyledon formation (18/30, 0/30 in controls) and aberrations in lateral organ positioning at inflorescence axes (25/62, 4/50 in controls; Figures 3C–3F). Moreover, PIN1:GFP reporter signals were reduced in *RP40p::gam* seedlings, while *PIN1* transcript levels appeared unaffected, indicating that ectopic *gam* expression interferes with post-transcriptional control of *PIN1* (Figures 3G–3I). To test whether *RP40p::gam* is affected in tRNA abundance, we determined steady-state levels of potential γ-toxin substrates, namely, tRNAs with a uridine at wobble position 34. In these experiments we normalized amounts of $tRNA^{Gln}_{UUG}$ and $tRNA^{Glu}_{UUC}$ to levels of $tRNA^{His}_{GUG}$ or $tRNA^{Ser}_{AGA}$, the latter two lacking a uridine at the wobble position, serving as internal standards (Figure 3B). We detected reduced abundance of $tRNA^{Gln}_{UUG}$ and $tRNA^{Glu}_{UUC}$ in *RP40p::gam* lines when compared to wild-type, suggesting that γ-toxin is active in *Arabidopsis* with substrate specificities similar to those observed in yeast.

Next, we tested for genetic interaction between Elongator and *RP40p::gam* by crossing *RP40p::gam* into *elp6*^{mop2} followed by analysis of the resulting progeny. Double homozygous *elp6*^{mop2} *RP40p::gam* strongly resembled parental *RP40p::gam* and *elp6*^{mop2} lines, which would be consistent with overlapping tRNA substrate specificities of Elongator and γ-toxin, when expressed in *Arabidopsis* (Figures S4A–S4F). However, *elp6*^{mop2} *RP40p::gam* appeared delayed in their development, when compared to parental lines (Figure S4G), indicating synergistic interaction between γ-toxin and Elongator, which points to an incomplete overlap of activities of these genetic traits.

We then tested *ELP* reporter constructs, stably transformed into *Arabidopsis*. Signals from functional *ELP6p::VENUS:ELP6* expressed in *elp6*^{mop2} were pronounced in stele, QC, and columella root cap cells, with weaker signals found in additional parts of the meristem (Figures 4B and 4C). Likewise in areal portions, the reporter appeared most abundant in the vasculature of developing organs (Figure 4A). At cellular resolution, VENUS:ELP6 signals were pronounced in the cytoplasm (Figure 4C). A similar cytoplasmic distribution along with nuclear signals was observed in *35S::YFP:ELP3* overexpression lines, while

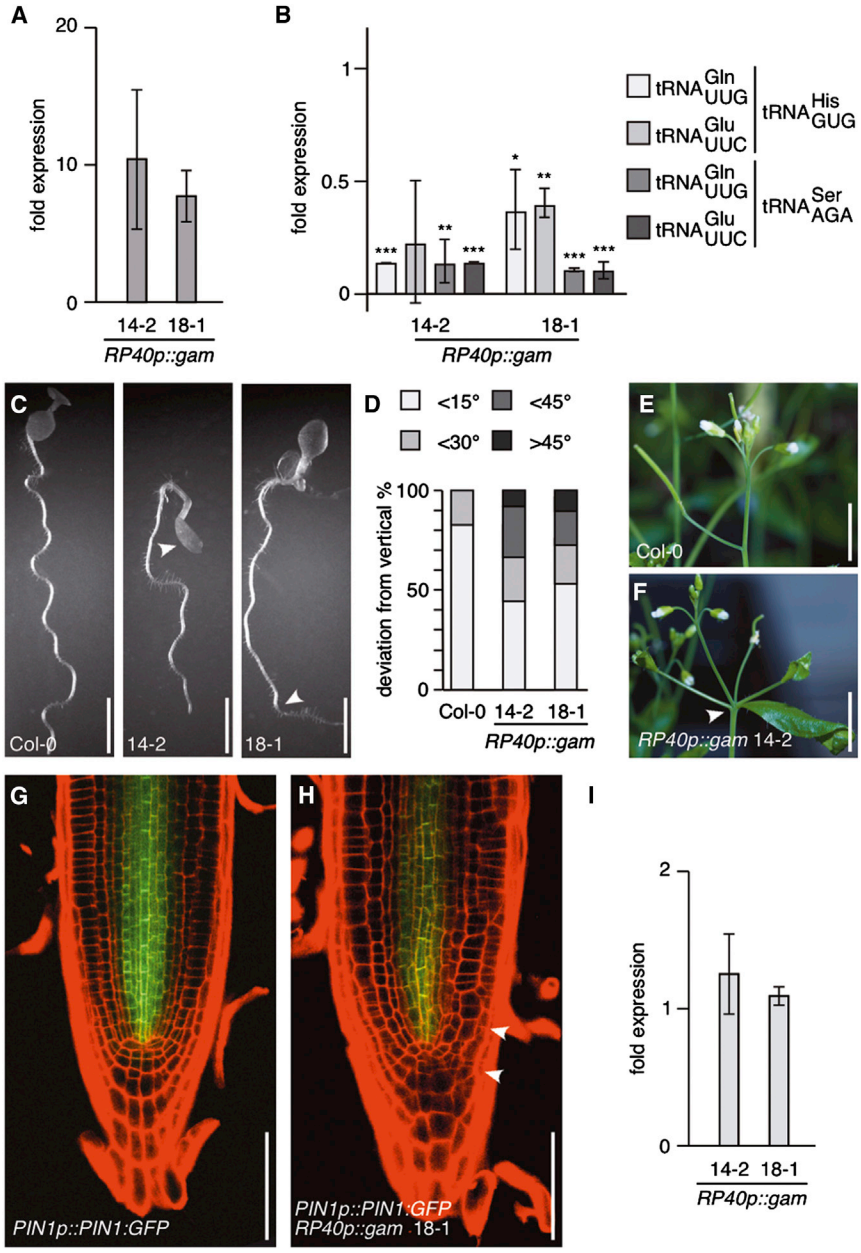

Figure 3. Expression of *Kluyveromyces lactis* γ-Toxin in *Arabidopsis* Downregulates Abundance of tRNAs and Causes Defects in Morphogenesis Resembling *elp* Mutants

(A) qPCR performed with cDNA from *RP40p::gam* lines 14-2 and 18-1. Transcript levels were normalized to expression of At5g60390 (= 1).

(B) qPCR displaying abundance of $tRNA^{Gln}_{UUG}$ and $tRNA^{Glu}_{UUC}$ in *Arabidopsis* seedlings at 5 DAG, after normalization to levels of either $tRNA^{His}_{GUG}$ or $tRNA^{Ser}_{AGA}$ as internal standards (relative tRNA abundance in Col-0 = 1). Results presented are obtained from two biological repeats each with three technical repeats. SDs are indicated (*t test < 0.05; **t test < 0.01; ***t test < 0.001).

(C) Comparison of Col-0 and *RP40p::gam* seedlings at 6 DAG. Alterations in cotyledon formation and directional root growth are indicated by white arrowheads.

(D) Orientation of primary root growth of Col-0 and *RP40p::gam* seedlings at 6 DAG. A total of 30–40 seedlings was analyzed for each data set and plotted as percentage of seedlings displaying <15°, <30°, <45°, and >45° deviation from the vertical growth axes.

(E and F) Comparison of Col-0 and *RP40p::gam* inflorescences at 35 DAG. White arrowhead: aberrations in inflorescence architecture.

(G and H) Expression of *PIN1::PIN1:GFP* (green) in Col-0 (G) and *RP40p::gam* (H) seedlings at 6 DAG. White arrowheads indicate aberrations in root patterning. Roots were stained with PI (red).

(I) qPCR displaying *PIN1* transcript levels in *RP40p::gam* lines 14-2 and 18-1 normalized to Col-0 (= 1). Results from three biological repeats with three technical replicates are shown.

SDs are indicated. Size bars represent 10 mm (C, E, and F) and 50 μm (G and H). See also Figure S4.

35S::YFP:GCN5, overexpressing a bona fide histone acetyltransferase, exclusively exhibited nuclear signals under our experimental conditions (compare Figures 4D–4F; Earley et al., 2007). Thus, analogous to observations made for Elongator in *S. cerevisiae*, cytoplasmic signals exhibited by *Arabidopsis* ELP reporter proteins are in agreement with a role of Elongator outside the nucleus and could involve a function in tRNA maturation (Huang et al., 2005; Rahl et al., 2005).

tRNA Processing as a General Determinant of Auxin Responses in Plants

Analysis of *elp* mutants and *RP40p::gam* point to a requirement of tRNA maturation for correct auxin responses. We asked whether this effect could be specific for tRNAs modified by Elongator or represents a more general response to alterations in tRNA homeostasis. We therefore analyzed *Arabidopsis RNA LIGASE* (*AtRNL*), a locus resembling yeast RNA ligase Trl1, implicated in splicing of tRNAs (Englert and Beier, 2005; Wang et al., 2006). In *Arabidopsis*, this would predominantly affect maturation of $tRNA^{Tyr}$, composed of a gene family of 76 loci, out of which 70 are predicted to contain an intron, whereas only a smaller sub-fraction of $tRNA^{Met}$ (11/24) and $tRNA^{Ser}$ (2/64) loci contains an intron (http://lowelab.ucsc.edu/GtRNAdb/Athal/). However, none of these tRNAs represents a likely target for Elongator, as they lack a uridine at their wobble position.

First, we analyzed expression of *AtRNLp::GUS* reporter transformed into *Arabidopsis* and found intense GUS staining in root meristems and in the vasculature of developing plantlets as well as in flowers and elongating tissue, pointing to a requirement for tRNA splicing preferentially in proliferating cell files and tissues (Figures S5A–S5G). Next, we sought for insertion mutants but

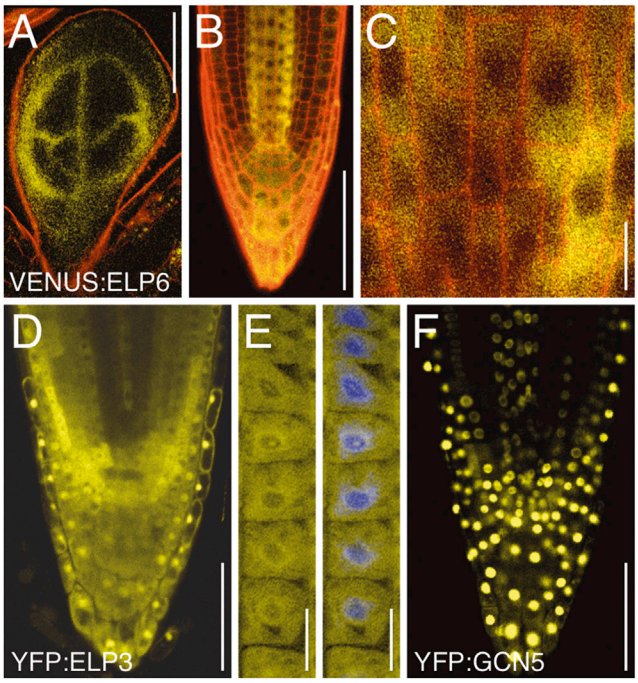

Figure 4. Expression Analysis of *ELP* Reporter Genes

(A and B) *ELP6p::VENUS:ELP6* expression (yellow) in developing true leaf (A) and primary root meristem (B) at 6 DAG.

(C) Cytoplasmic distribution of *ELP6p::VENUS:ELP6* in root meristem stele cells. Areas with reduced signal intensities represent nuclei. Seedlings were stained with PI (red) to visualize cell and organ boundaries.

(D) Expression of *35S::YFP:ELP3* (yellow signals) in 6-day-old Col-0 root meristem cells results in cytoplasmic and additional nuclear signals.

(E) *35S::YFP:ELP3* root meristem epidermis cells (6 DAG) displaying pronounced cytoplasmic signals. To visualize nuclei, seedlings were fixed and counterstained with DAPI (blue).

(F) Expression of *35S::YFP:GCN5*, encoding a nuclear-localized protein, in Col-0 root meristem cells under conditions identical to those in (D).

Size bars represent 100 μm (A), 50 μm (B, D, and F), and 10 μm (C and E).

failed to obtain lines with noticeable effects on *AtRNL* gene expression (see the Supplemental Information). We therefore took another approach and generated artificial microRNA lines (Schwab et al., 2006), in which transcription of endogenous *AtRNL* was downregulated (Figure 5A; Figures S6A and S6B). When determining splicing of $tRNA^{Tyr}_{GUA}$ in *RP40p::amiRNL-b* seedlings at 5 days after germination (DAG), we detected a strong reduction in the amounts of processed tRNA, suggesting that these plants contain only limited quantities of functional $tRNA^{Tyr}$ due to deficiencies in the splicing reaction (Figure 5B).

Morphology and development of *RP40p::amiRNL-b* resembled those of *elp/mop* mutants (10/16 lines analyzed). Specifically, *RP40p::amiRNL-b* seedlings exhibited reduced root elongation, aberrations in cotyledon number (49/91; 1/35 in Col-0) and incomplete cotyledon venation (17/40; 0/35 in Col-0) as well as deficiencies in root meristem morphology and root gravitropism (Figures 5C–5E, 5J, and 5K). At later developmental stages, we observed reduced apical dominance and aberrations in lateral organ positioning at inflorescence stems (27/62; 2/38 in Col-0; Figures 5H and 5I). Related growth defects have been linked to alterations in auxin responses, and we therefore analyzed expression of auxin responsive $DR5_{rev}$*::GFP* (Benková et al., 2003). Reporter signals in *RP40p::amiRNL-b* $DR5_{rev}$*::GFP* primary root meristems appeared reduced (Figures 5J and 5K), indicating alterations in auxin distribution and/or signaling that coincide with deficiencies in tRNA splicing.

To validate our observations, we generated another *amiRNL* construct, expressed under control of the 35S promoter, and targeting a different region of the *AtRNL* mRNA. Transgenic *35S::amiRNL-a* seedlings with reduced abundance of *AtRNL* transcript exhibited phenotypes resembling those of *RP40p::amiRNL-b* (Figures S6B–S6F). This corroborates a scenario in which phenotypes observed result from downregulation of *AtRNL* and associated aberrations in tRNA splicing. Moreover, the resemblance of *amiRNL* and *elp* loss-of-function mutants, both predicted to impact on distinct sets of tRNA families, indicates that non-overlapping limitations in tRNA availability give rise to comparable developmental defects.

tRNA Maturation Acts in the Transmission of Instructive Auxin Cues

To further define the role of Elongator and *AtRNL* in auxin-controlled morphogenesis, we analyzed lateral root formation, a process that depends on coordinated distribution of auxin (Benková et al., 2003). When viewing *AtRNLp::GUS* activity, GUS staining became visible already in stage I lateral root primordia, and strong expression remained detectable during later stages of organ development (Figures 6A and 6B). Likewise, in $elp6^{mop2}$ *ELP6p::VENUS:ELP6* signals became detectable upon primordium development and remained visible during further growth (Figures 6C and 6D). This points to a function for Elongator and *AtRNL* in lateral root growth, and we next determined expression of *PIN1p::PIN1:GFP* in lateral roots of wild-type, $elp6^{mop2}$, and *RP40p::amiRNL-b* seedlings. PIN1:GFP signals in $elp6^{mop2}$ turned out to be weaker than in wild-type, and similar findings were made, when analyzing reporter signals in *RP40p::amiRNL-b* lateral roots (compare Figures 6E–6J). Thus, as observed for primary root meristems (Figure 1; Figures S6G–S6I), *PIN1* expression appears reduced in lateral roots upon interference with tRNA maturation.

We then tested for possible consequences of reduced PIN expression and compared lateral root growth in wild-type and $elp6^{mop2}$. This revealed a reduction in the number of $elp6^{mop2}$ lateral roots, when compared to wild-type (Figure 6K). When analyzing *RP40p::amiRNL-b*, we observed a reduction in lateral root formation as well, but effects in the silencer lines appeared less pronounced and more variable than in $elp6^{mop2}$ (Figure 6K). When performing root growth experiments in the presence of low concentrations of the auxin analog 1-napthalene acetic acid (NAA) without noticeable effects on lateral root growth in wild-type, we detected rescue of lateral root formation specifically in $elp6^{mop2}$ (Figure 6K). This is in accordance with limitations in auxin availability and/or distribution causing lateral root growth deficiencies associated with the mutant, and consistent with a role of Elongator in transmission of instructive auxin signals during root morphogenesis. Taken together, our findings link tRNA maturation to root organogenesis, potentially via mechanisms

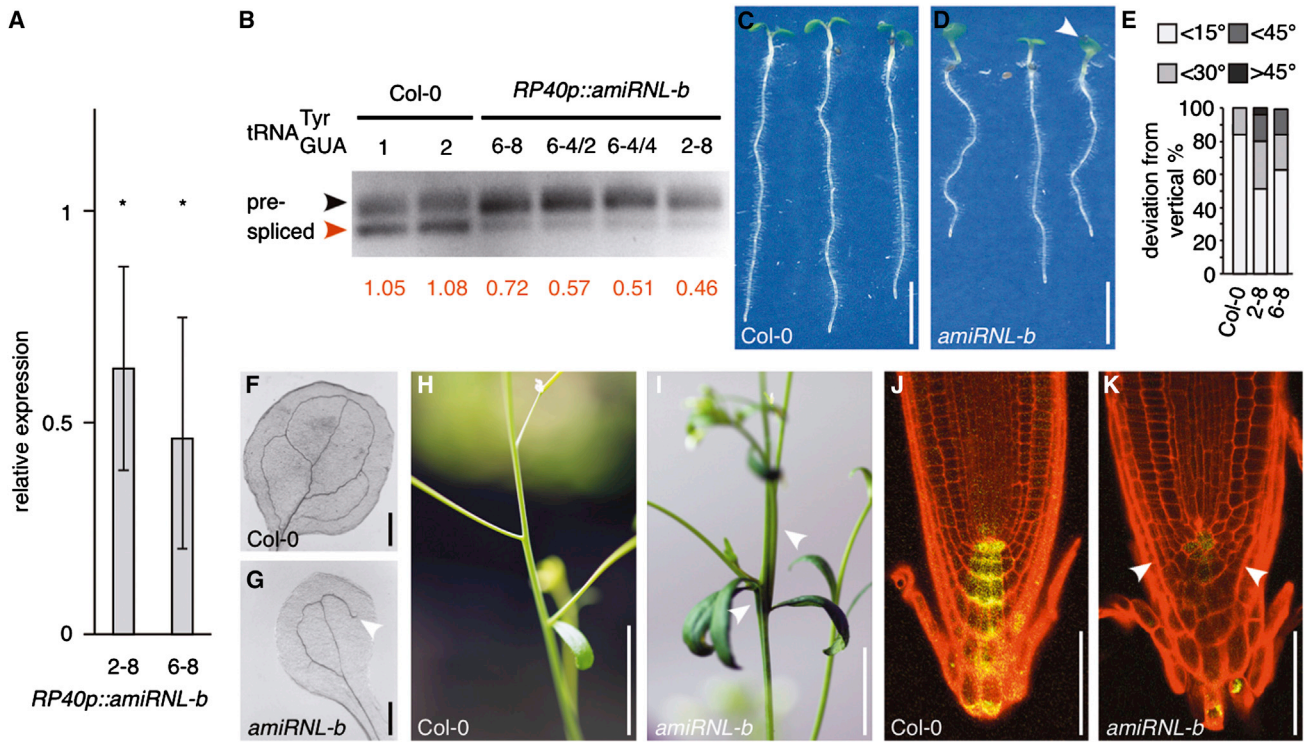

Figure 5. Analysis of *AtRNL* RNA Ligase Knockdown Lines

(A) qPCR displaying *AtRNL* transcript levels in *RP40p:amiRNL-b* lines 2–8 and 6–8 at 6 DAG (Col-0 = 1). Results from three biological repeats with three technical replicates are shown. SDs are indicated (*Student's two-tailed t test, $p < 0.01$).

(B) Quantification of $tRNA^{Tyr}_{GUA}$ levels in Col-0 and *RP40p::amiRNL-b* silencer lines by PCR. Upper band corresponds to non-spliced $tRNA^{Tyr}_{GUA}$ precursor (black arrowhead); lower band corresponds to processed $tRNA^{Tyr}_{GUA}$ (red arrowhead). Ratios of spliced and precursor band intensities are displayed below.

(C and D) Col-0 (C) and *RP40p::amiRNL-b* (D) seedlings at 6 DAG. White arrowhead in (D) points to fused cotyledons.

(E) Orientation of primary root growth of Col-0 and *RP40p::amiRNL-b* lines 2–8 and 6–8 seedlings at 8 DAG. A total of 40–50 seedlings was analyzed for each genotype and plotted as percentage of seedlings displaying <15°, <30°, <45°, and >45° deviation from the vertical growth axes.

(F and G) Cotyledon vasculature in Col-0 (F) and *RP40p::amiRNL-b* (G). White arrowhead indicates vasculature discontinuity not observed in wild-type.

(H and I) Detail of inflorescence axes of flowering Col-0 (H) and *RP40p::amiRNL-b* (I) at 28 DAG. White arrowheads indicate fused, fasciated stem.

(J and K) Comparison of wild-type (J) and *RP40p::amiRNL-b* (K) primary root meristems expressing auxin-responsive $DR5_{rev}$*::GFP* (yellow). Roots were stained with PI (red) to visualize cell boundaries. White arrowheads point to alterations in root meristem patterning.

Size bars represent 10 mm (C, D, H, and I), 1 mm (F and G), and 50 μm (J and K). See also Figures S5 and S6.

orchestrating PIN activities and associated adjustments in auxin distribution.

DISCUSSION

Recent years have seen characterization of a range of signaling pathways in higher plants, revealing molecular switches that communicate signals essential for plant development. Auxin appears to be transmitted by distinct pathways, with $SCF^{TIR1/AFB}$-dependent hormone perception predominantly affecting transcriptional control (Dharmasiri et al., 2005; Kepinski and Leyser, 2005). Another pathway, suggested to modulate protein sorting in response to auxin, seemingly requires ROP-GTPase activity (Paciorek et al., 2005; Xu et al., 2010), while involvement of putative auxin receptor auxin binding protein 1 in auxin-controlled development has been seriously challenged very recently (Gao et al., 2015). The identification of components acting in auxin signaling provided insights into principles that might confer specificity to such hormonal responses, but additional reports demonstrated that less specific cellular processes contribute to the orchestration of auxin effects as well (Dhonukshe et al., 2008; Kitakura et al., 2011; Korbei et al., 2013; Rosado et al., 2010, 2012; Wang et al., 2013a). Our findings establish tRNA maturation as a highly general effector of auxin responses, acting via translational control of PIN proteins, and provoking questions on function and specificity of such activities in the regulation of hormonal signaling (Retzer et al., 2014).

Elongator has been linked to diverse cellular activities ranging from gene expression to protein sorting, which seemingly depends on integrity of the protein complex, as loss of individual *ELP* loci causes essentially identical defects (Chen et al., 2009; Esberg et al., 2006; Frohloff et al., 2001; Huang et al., 2005; Nelissen et al., 2005; Otero et al., 1999; Rahl et al., 2005; Singh et al., 2010; Wittschieben et al., 1999; Xu et al., 2012). Evidence for ELP acting particularly in tRNA modification came from studies in yeast, demonstrating that selective overexpression

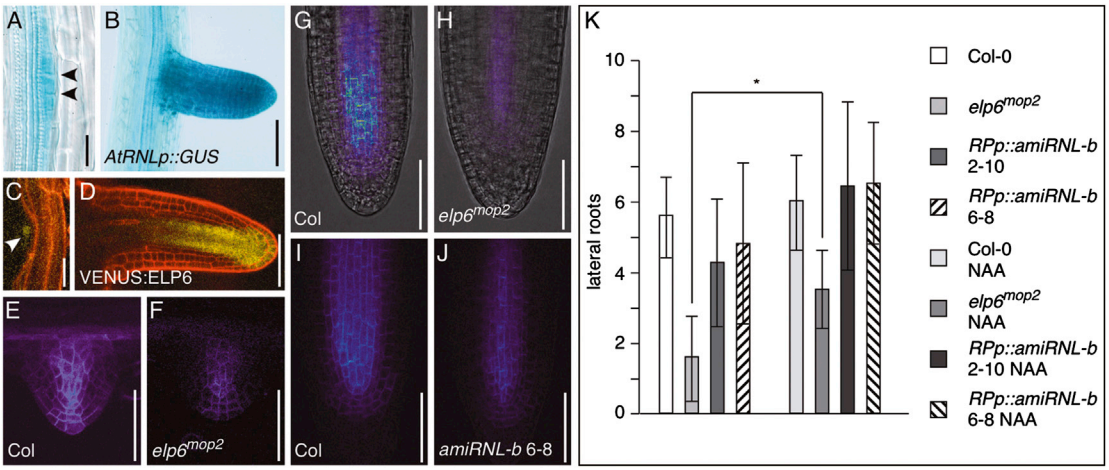

Figure 6. Elongator and *AtRNL* during Lateral Root Formation

(A and B) *AtRNLp::GUS* activity at early (A) and later (B) stages of lateral root development. Arrowheads point to early-stage lateral root primordium.

(C and D) *ELP6p::VENUS:ELP6* expression (yellow) at early (C, white arrowhead) and later (D) stages of lateral root development. Roots were counterstained with PI to visualize cell boundaries.

(E–H) *PIN1p::PIN1:GFP* signals in Col-0 (E and G) and *elp6*^{mop2} (F and H) at early (E and F) and later (G and H) stages of lateral root development.

(I and J) Expression of *PIN1p::PIN1:GFP* in lateral roots of Col-0 (I) and *RP40p::amiRNL-b* (J).

(K) Number of lateral roots formed by Col-0, *elp6*^{mop2}, and *RP40p::amiRNL-b* at 10 DAG (*Student's two-tailed t test; $p < 0.001$; n = 25–30 for each genotype and condition).

Size bars represent 15 μm (A), 50 μm (B, D, and E–J), and 25 μm (C). See also Figure S6.

of two individual tRNAs can bypass major *elp* mutant phenotypes, presumably via compensating for the loss of translational fidelity that results from defects in Elongator (Esberg et al., 2006). Another link between Elongator and tRNA modifications came from crystallization of the ELP4/5/6 sub-complex (Glatt et al., 2012; Lin et al., 2012). These studies revealed a hexameric ring-shaped structure capable of interacting with the tRNA anticodon loop domain, which presumably represents a topological prerequisite for ELP-mediated ribonucleotide modification (Glatt et al., 2012). Moreover, analysis of protein abundance in an *Schizosaccharomyces pombe Δelp3* mutant linked codon usage and Elongator-dependent variations in translational efficiency to discrete growth defects (Bauer et al., 2012). From all that, it seems that tRNA modification represents a major enzymatic function of Elongator (Glatt and Müller, 2013).

Like its fungal counterpart, *Arabidopsis* Elongator appears to function in diverse processes, including stress response, pathogen defense, and hormonal signaling, which has been attributed to Elongator's activities in chromatin modification and transcriptional control (Chen et al., 2006; Nelissen et al., 2010; Sanmartín et al., 2011; Wang et al., 2013b; Zhou et al., 2009). Our results now establish links between Elongator-mediated tRNA modification and auxin-controlled pattern formation. Apart from reduced uridine modifications in tRNA preparations of *elp/mop* mutants, phenotypes observed upon expression of γ-toxin in *Arabidopsis* further substantiate such a role. Experiments in baker's yeast demonstrated that tRNAs featuring mcm^{5}s^{2}U or ncm^{5}U at their wobble position represent preferred targets for γ-toxin (Lu et al., 2005), and our results point to related γ-toxin substrate specificities in *Arabidopsis*. In accordance, we observed comparable phenotypes when analyzing *elp/mop* mutants and *RP40p::gam* lines, which is consistent with overlapping tRNA substrate specificities of *Arabidopsis* Elongator and γ-toxin. Notably, although displaying phenotypes as their parental lines, growth of *elp6*^{mop2} *RP40p::gam* plants turned out to be retarded, when compared to its parents. Such additive phenotypes argue for an incomplete overlap in the activity of *Arabidopsis ELP6* and γ-toxin. Alternatively, remaining tRNA modification activities in either *elp6*^{mop2} or *RP40p::gam* could be reduced further in *elp6*^{mop2} *RP40p::gam* plants. Whether these synergistic phenotypes reflect diverging activities in tRNA substrate processing or activities even unrelated to tRNA modifications remains to be addressed.

One might speculate about a function of Elongator in translational control, primarily required for the transmission of auxin signals. Limited PIN abundance in Elongator mutants, together with the finding that efficient overexpression of *PIN1* partially rescues *elp6*^{mop2} growth defects, is in fact consistent with this model. Analysis of *AtRNL*, however, argues against such a scenario but rather implies less specific effects of tRNA availability on auxin-controlled growth and differentiation processes. The *Arabidopsis* tRNA$^{Tyr}_{GUA}$ family likely represents a major substrate for the *AtRNL* RNA-ligase, indicated by pronounced deficiencies in tRNA^{Tyr} splicing in *amiRNL* lines. In addition, members of the tRNA$^{Met}_{CAU}$ and tRNA$^{Ser}_{GCU}$ families represent potential *AtRNL* substrates, but none of these tRNAs is a likely target of Elongator, as they all lack uridine at wobble position 34. While this implies differing tRNA substrate specificities for Elongator and *AtRNL*, loss of either *ELP* or *AtRNL* still causes similar phenotypes, which points to a requirement of these distinct regulators of translational control in overlapping aspects of plant development.

Broad deficiencies in tRNA biogenesis as apparent in *elp/mop* and *amiRNL* should result in major changes in translational control, with reduced abundance of PINs representing only a small fraction of aberrations in protein translation. This would be in agreement with the various functions in signaling and stress responses attributed to *Arabidopsis* Elongator. In light of such diverse activities, it seems remarkable that several developmental defects associated with *elp/mop* mutants could be explained essentially by aberrations in auxin-controlled morphogenesis. Another report, linking tRNA function to auxin, described identification of an auxin response mutant, which turned out to be affected in a member of the $tRNA^{Ala}_{CGC}$ family (Perry et al., 2005). This mutant is predicted to erroneously and stochastically incorporate valine instead of alanine into growing peptide chains, nonetheless resulting in discrete defects in mediating auxin effects on cell proliferation (Perry et al., 2005). It remains to be determined how altered decoding characteristics of a single tRNA could give rise to such defined growth defects, which is all the more surprising as the *Arabidopsis* genome is predicted to encode 630 tRNAs, strongly suggestive of extensive functional redundancy (http://lowelab.ucsc.edu/GtRNAdb/Athal/).

The importance of tRNA maturation specifically for auxin responses and cell proliferation is underlined by our study, indicative of a high demand for *AtRNL* and Elongator activities in metabolically active and proliferating tissue. Limitations in the availability of tRNAs, as is the case for Elongator loss-of-function or *AtRNL* knockdown alleles, would translate into variations in the abundance of various proteins, including key mediators of plant development and pattern formation. PIN proteins seemingly represent such targets, as interference with tRNA maturation impacts on PIN levels, coinciding with modifications in auxin distribution and developmental reprogramming, which is reflected in major adjustments in proliferative growth. Rescue of $elp6^{mop2}$ lateral root growth defects by auxin supports such a scenario, as it indicates that aberrations in auxin availability or distribution are indeed accountable for *elp/mop* growth defects.

A plausible explanation for our observations implies that components of the auxin transport and/or signaling machinery represent rate-limiting determinants for plant morphogenesis. This is underlined by rescue of *elp/mop* root phenotypes via efficient *PIN1* overexpression, likely compensating for suboptimal translation as a result of limiting availability of fully processed tRNAs. Related models have been put forward when studying fundamental aspects of cellular activity, including cytoskeleton function, endocytic protein sorting, and ribosome biogenesis, perturbation of which consistently resulted in phenotypes that could be linked to altered auxin responses (Dhonukshe et al., 2008; Kitakura et al., 2011; Retzer et al., 2014; Rosado et al., 2010; Wang et al., 2013a; Zhou et al., 2010). While none of these processes represents an integral element of auxin signaling pathways, it appears that plant cells have evolved mechanisms, conferring signaling specificity by means of highly general regulatory events. ROP-GTPases modulate intracellular sorting of PIN plasma membrane proteins and hence distribution of auxin (Xu et al., 2010). Moreover, activity of ribosome-associated proteins appears indispensable for translational re-initiation of *ARF* mRNAs, which contain regulatory uORFs, upstream of their actual Start-ATG (Rosado et al., 2012). However, such translational re-initiation is not restricted to transcriptional regulators of auxin responses, as about one-third of *Arabidopsis* protein-coding mRNAs is predicted to contain regulatory uORFs (von Arnim et al., 2014). Likewise, ROP activity is assumed to exert general effects on plasma membrane protein sorting not limited to auxin transport components, underpinning the role of PINs as well as additional elements of the auxin signaling machinery as a limiting bottleneck for plant development.

Insights into the mechanisms controlling tRNA maturation in higher plants are just emerging, which should contribute to our understanding of their function in plant development (Chen et al., 2010). Adjustments in tRNA maturation could, for example, arise as a consequence of variations in environmental parameters, causing modifications in translational control. In this scenario, reversible changes in the abundance of PIN auxin transport proteins resulting from fluctuations in translational efficiency would link fundamental cellular activities to defined events in pattern formation and morphogenesis. This would allow for efficient and rapid transmission of morphogenetic cues, simply by exploiting the rate-limiting role of auxin signaling for plant development. Experiments addressing environmental parameters and its effects on translational control are required to further test this hypothesis.

EXPERIMENTAL PROCEDURES

Plant Growth and Lines

Seedlings were cultured and analyzed as described (Korbei et al., 2013), in a 16-hr-light/8-hr-dark regimen at 22°C, unless indicated differently.

Generation of Constructs and Expression Analysis

Construct cloning and plant transformation was performed according to established protocols (Butt et al., 2014). Sample preparation and expression analysis has been described elsewhere (Butt et al., 2014; Korbei et al., 2013).

Microscopy

Seedlings were analyzed on Leica confocal laser scanning microscopes (CLSMs) as described (Korbei et al., 2013). A detailed description of all experimental procedures is provided as Supplemental Information.

SUPPLEMENTAL INFORMATION

Supplemental Information includes Supplemental Experimental Procedures, six figures, and one table and can be found with this article online at http://dx.doi.org/10.1016/j.celrep.2015.03.054.

AUTHOR CONTRIBUTIONS

J.L., N.M., R.B., D. L., C.L., and B.K. performed analysis of Elongator mutants and reporter lines. J.L., C.L., and K.R. analyzed γ-toxin lines; K.R. generated and analyzed *amiRNL* lines. G.J. and A. B. assessed tRNA modifications in *elp* mutants. A.B and C.L. conceived experiments, and C.L. wrote the manuscript.

ACKNOWLEDGMENTS

This work was supported by grants from the Austrian Science Funds (FWF; P19585 and P25931 to C.L.; T477 to B.K.) and a Docfforte fellowship from the Austrian Academy of Sciences to K.R. A.S.B. is supported by grants from the Swedish Cancer Foundation (13 0301), Swedish Research Council (621-2012-3576), and Karin and Harald Silvanders Foundation (223-2808-12). We are indebted to Eva Benkova, Niko Geldner, Toru Fujiwara, and Craig Pikaard for providing published materials.

Received: August 21, 2014
Revised: March 2, 2015
Accepted: March 25, 2015
Published: April 16, 2015

REFERENCES

Bauer, F., Matsuyama, A., Candiracci, J., Dieu, M., Scheliga, J., Wolf, D.A., Yoshida, M., and Hermand, D. (2012). Translational control of cell division by Elongator. Cell Rep. *1*, 424–433.

Benková, E., Michniewicz, M., Sauer, M., Teichmann, T., Seifertová, D., Jürgens, G., and Friml, J. (2003). Local, efflux-dependent auxin gradients as a common module for plant organ formation. Cell *115*, 591–602.

Boer, D.R., Freire-Rios, A., van den Berg, W.A., Saaki, T., Manfield, I.W., Kepinski, S., López-Vidrieo, I., Franco-Zorrilla, J.M., de Vries, S.C., Solano, R., et al. (2014). Structural basis for DNA binding specificity by the auxin-dependent ARF transcription factors. Cell *156*, 577–589.

Butt, H., Graner, S., and Luschnig, C. (2014). Expression analysis of Arabidopsis XH/XS-domain proteins indicates overlapping and distinct functions for members of this gene family. J. Exp. Bot. *65*, 1217–1227.

Chen, Z., Zhang, H., Jablonowski, D., Zhou, X., Ren, X., Hong, X., Schaffrath, R., Zhu, J.K., and Gong, Z. (2006). Mutations in ABO1/ELO2, a subunit of holo-Elongator, increase abscisic acid sensitivity and drought tolerance in Arabidopsis thaliana. Mol. Cell. Biol. *26*, 6902–6912.

Chen, C., Tuck, S., and Byström, A.S. (2009). Defects in tRNA modification associated with neurological and developmental dysfunctions in Caenorhabditis elegans elongator mutants. PLoS Genet. *5*, e1000561.

Chen, P., Jäger, G., and Zheng, B. (2010). Transfer RNA modifications and genes for modifying enzymes in Arabidopsis thaliana. BMC Plant Biol. *10*, 201.

Dharmasiri, N., Dharmasiri, S., and Estelle, M. (2005). The F-box protein TIR1 is an auxin receptor. Nature *435*, 441–445.

Dhonukshe, P., Grigoriev, I., Fischer, R., Tominaga, M., Robinson, D.G., Hasek, J., Paciorek, T., Petrásek, J., Seifertová, D., Tejos, R., et al. (2008). Auxin transport inhibitors impair vesicle motility and actin cytoskeleton dynamics in diverse eukaryotes. Proc. Natl. Acad. Sci. USA *105*, 4489–4494.

Earley, K.W., Shook, M.S., Brower-Toland, B., Hicks, L., and Pikaard, C.S. (2007). In vitro specificities of Arabidopsis co-activator histone acetyltransferases: implications for histone hyperacetylation in gene activation. Plant J. *52*, 615–626.

Englert, M., and Beier, H. (2005). Plant tRNA ligases are multifunctional enzymes that have diverged in sequence and substrate specificity from RNA ligases of other phylogenetic origins. Nucleic Acids Res. *33*, 388–399.

Esberg, A., Huang, B., Johansson, M.J., and Byström, A.S. (2006). Elevated levels of two tRNA species bypass the requirement for elongator complex in transcription and exocytosis. Mol. Cell *24*, 139–148.

Frohloff, F., Fichtner, L., Jablonowski, D., Breunig, K.D., and Schaffrath, R. (2001). Saccharomyces cerevisiae Elongator mutations confer resistance to the Kluyveromyces lactis zymocin. EMBO J. *20*, 1993–2003.

Gao, Y., Zhang, Y., Zhang, D., Dai, X., Estelle, M., and Zhao, Y. (2015). Auxin binding protein 1 (ABP1) is not required for either auxin signaling or Arabidopsis development. Proc. Natl. Acad. Sci. USA *112*, 2275–2280.

Glatt, S., and Müller, C.W. (2013). Structural insights into Elongator function. Curr. Opin. Struct. Biol. *23*, 235–242.

Glatt, S., Létoquart, J., Faux, C., Taylor, N.M., Séraphin, B., and Müller, C.W. (2012). The Elongator subcomplex Elp456 is a hexameric RecA-like ATPase. Nat. Struct. Mol. Biol. *19*, 314–320.

Hawkes, N.A., Otero, G., Winkler, G.S., Marshall, N., Dahmus, M.E., Krappmann, D., Scheidereit, C., Thomas, C.L., Schiavo, G., Erdjument-Bromage, H., et al. (2002). Purification and characterization of the human elongator complex. J. Biol. Chem. *277*, 3047–3052.

Huang, B., Johansson, M.J., and Byström, A.S. (2005). An early step in wobble uridine tRNA modification requires the Elongator complex. RNA *11*, 424–436.

Johansson, M.J., Esberg, A., Huang, B., Björk, G.R., and Byström, A.S. (2008). Eukaryotic wobble uridine modifications promote a functionally redundant decoding system. Mol. Cell. Biol. *28*, 3301–3312.

Kepinski, S., and Leyser, O. (2005). The Arabidopsis F-box protein TIR1 is an auxin receptor. Nature *435*, 446–451.

Kitakura, S., Vanneste, S., Robert, S., Löfke, C., Teichmann, T., Tanaka, H., and Friml, J. (2011). Clathrin mediates endocytosis and polar distribution of PIN auxin transporters in Arabidopsis. Plant Cell *23*, 1920–1931.

Korbei, B., Moulinier-Anzola, J., De-Araujo, L., Lucyshyn, D., Retzer, K., Khan, M.A., and Luschnig, C. (2013). Arabidopsis TOL proteins act as gatekeepers for vacuolar sorting of PIN2 plasma membrane protein. Curr. Biol. *23*, 2500–2505.

Leitner, J. (2011). Ubiquitylation and translational fidelity as regulatory cues for Arabidopsis thaliana PIN proteins (Wien: Universitat fur Bodenkultur Wien).

Lin, Z., Zhao, W., Diao, W., Xie, X., Wang, Z., Zhang, J., Shen, Y., and Long, J. (2012). Crystal structure of elongator subcomplex Elp4-6. J. Biol. Chem. *287*, 21501–21508.

Ljung, K. (2013). Auxin metabolism and homeostasis during plant development. Development *140*, 943–950.

Lu, J., Huang, B., Esberg, A., Johansson, M.J., and Byström, A.S. (2005). The Kluyveromyces lactis gamma-toxin targets tRNA anticodons. RNA *11*, 1648–1654.

Malenica, N., Abas, L., Benjamins, R., Kitakura, S., Sigmund, H.F., Jun, K.S., Hauser, M.T., Friml, J., and Luschnig, C. (2007). MODULATOR OF PIN genes control steady-state levels of Arabidopsis PIN proteins. Plant J. *51*, 537–550.

Mehlgarten, C., Jablonowski, D., Wrackmeyer, U., Tschitschmann, S., Sondermann, D., Jäger, G., Gong, Z., Byström, A.S., Schaffrath, R., and Breunig, K.D. (2010). Elongator function in tRNA wobble uridine modification is conserved between yeast and plants. Mol. Microbiol. *76*, 1082–1094.

Nelissen, H., Fleury, D., Bruno, L., Robles, P., De Veylder, L., Traas, J., Micol, J.L., Van Montagu, M., Inzé, D., and Van Lijsebettens, M. (2005). The elongata mutants identify a functional Elongator complex in plants with a role in cell proliferation during organ growth. Proc. Natl. Acad. Sci. USA *102*, 7754–7759.

Nelissen, H., De Groeve, S., Fleury, D., Neyt, P., Bruno, L., Bitonti, M.B., Vandenbussche, F., Van der Straeten, D., Yamaguchi, T., Tsukaya, H., et al. (2010). Plant Elongator regulates auxin-related genes during RNA polymerase II transcription elongation. Proc. Natl. Acad. Sci. USA *107*, 1678–1683.

Otero, G., Fellows, J., Li, Y., de Bizemont, T., Dirac, A.M., Gustafsson, C.M., Erdjument-Bromage, H., Tempst, P., and Svejstrup, J.Q. (1999). Elongator, a multisubunit component of a novel RNA polymerase II holoenzyme for transcriptional elongation. Mol. Cell *3*, 109–118.

Paciorek, T., Zazímalová, E., Ruthardt, N., Petrásek, J., Stierhof, Y.D., Kleine-Vehn, J., Morris, D.A., Emans, N., Jürgens, G., Geldner, N., and Friml, J. (2005). Auxin inhibits endocytosis and promotes its own efflux from cells. Nature *435*, 1251–1256.

Peer, W.A., Blakeslee, J.J., Yang, H., and Murphy, A.S. (2011). Seven things we think we know about auxin transport. Mol. Plant *4*, 487–504.

Perry, J., Dai, X., and Zhao, Y. (2005). A mutation in the anticodon of a single tRNAala is sufficient to confer auxin resistance in Arabidopsis. Plant Physiol. *139*, 1284–1290.

Petrásek, J., Mravec, J., Bouchard, R., Blakeslee, J.J., Abas, M., Seifertová, D., Wisniewska, J., Tadele, Z., Kubes, M., Covanová, M., et al. (2006). PIN proteins perform a rate-limiting function in cellular auxin efflux. Science *312*, 914–918.

Rahl, P.B., Chen, C.Z., and Collins, R.N. (2005). Elp1p, the yeast homolog of the FD disease syndrome protein, negatively regulates exocytosis independently of transcriptional elongation. Mol. Cell *17*, 841–853.

Retzer, K., Butt, H., Korbei, B., and Luschnig, C. (2014). The far side of auxin signaling: fundamental cellular activities and their contribution to a defined growth response in plants. Protoplasma *251*, 731–746.

Rosado, A., Sohn, E.J., Drakakaki, G., Pan, S., Swidergal, A., Xiong, Y., Kang, B.H., Bressan, R.A., and Raikhel, N.V. (2010). Auxin-mediated ribosomal

biogenesis regulates vacuolar trafficking in Arabidopsis. Plant Cell *22*, 143–158.

Rosado, A., Li, R., van de Ven, W., Hsu, E., and Raikhel, N.V. (2012). Arabidopsis ribosomal proteins control developmental programs through translational regulation of auxin response factors. Proc. Natl. Acad. Sci. USA *109*, 19537–19544.

Sanmartín, M., Sauer, M., Muñoz, A., Zouhar, J., Ordóñez, A., van de Ven, W.T., Caro, E., de la Paz Sánchez, M., Raikhel, N.V., Gutiérrez, C., et al. (2011). A molecular switch for initiating cell differentiation in Arabidopsis. Curr. Biol. *21*, 999–1008.

Sauer, M., Robert, S., and Kleine-Vehn, J. (2013). Auxin: simply complicated. J. Exp. Bot. *64*, 2565–2577.

Schwab, R., Ossowski, S., Riester, M., Warthmann, N., and Weigel, D. (2006). Highly specific gene silencing by artificial microRNAs in Arabidopsis. Plant Cell *18*, 1121–1133.

Sieberer, T., Hauser, M.T., Seifert, G.J., and Luschnig, C. (2003). PROPORZ1, a putative Arabidopsis transcriptional adaptor protein, mediates auxin and cytokinin signals in the control of cell proliferation. Curr. Biol. *13*, 837–842.

Singh, N., Lorbeck, M.T., Zervos, A., Zimmerman, J., and Elefant, F. (2010). The histone acetyltransferase Elp3 plays in active role in the control of synaptic bouton expansion and sleep in Drosophila. J. Neurochem. *115*, 493–504.

Takano, J., Miwa, K., Yuan, L., von Wirén, N., and Fujiwara, T. (2005). Endocytosis and degradation of BOR1, a boron transporter of Arabidopsis thaliana, regulated by boron availability. Proc. Natl. Acad. Sci. USA *102*, 12276–12281.

Ulmasov, T., Hagen, G., and Guilfoyle, T.J. (1999). Activation and repression of transcription by auxin-response factors. Proc. Natl. Acad. Sci. USA *96*, 5844–5849.

von Arnim, A.G., Jia, Q., and Vaughn, J.N. (2014). Regulation of plant translation by upstream open reading frames. Plant Sci. *214*, 1–12.

Voß, U., Bishopp, A., Farcot, E., and Bennett, M.J. (2014). Modelling hormonal response and development. Trends Plant Sci. *19*, 311–319.

Wabnik, K., Govaerts, W., Friml, J., and Kleine-Vehn, J. (2011). Feedback models for polarized auxin transport: an emerging trend. Mol. Biosyst. *7*, 2352–2359.

Wang, L.K., Schwer, B., Englert, M., Beier, H., and Shuman, S. (2006). Structure-function analysis of the kinase-CPD domain of yeast tRNA ligase (Trl1) and requirements for complementation of tRNA splicing by a plant Trl1 homolog. Nucleic Acids Res. *34*, 517–527.

Wang, C., Yan, X., Chen, Q., Jiang, N., Fu, W., Ma, B., Liu, J., Li, C., Bednarek, S.Y., and Pan, J. (2013a). Clathrin light chains regulate clathrin-mediated trafficking, auxin signaling, and development in Arabidopsis. Plant Cell *25*, 499–516.

Wang, Y., An, C., Zhang, X., Yao, J., Zhang, Y., Sun, Y., Yu, F., Amador, D.M., and Mou, Z. (2013b). The Arabidopsis elongator complex subunit2 epigenetically regulates plant immune responses. Plant Cell *25*, 762–776.

Winkler, G.S., Petrakis, T.G., Ethelberg, S., Tokunaga, M., Erdjument-Bromage, H., Tempst, P., and Svejstrup, J.Q. (2001). RNA polymerase II elongator holoenzyme is composed of two discrete subcomplexes. J. Biol. Chem. *276*, 32743–32749.

Wittschieben, B.O., Otero, G., de Bizemont, T., Fellows, J., Erdjument-Bromage, H., Ohba, R., Li, Y., Allis, C.D., Tempst, P., and Svejstrup, J.Q. (1999). A novel histone acetyltransferase is an integral subunit of elongating RNA polymerase II holoenzyme. Mol. Cell *4*, 123–128.

Xu, T., Wen, M., Nagawa, S., Fu, Y., Chen, J.G., Wu, M.J., Perrot-Rechenmann, C., Friml, J., Jones, A.M., and Yang, Z. (2010). Cell surface- and rho GTPase-based auxin signaling controls cellular interdigitation in Arabidopsis. Cell *143*, 99–110.

Xu, D., Huang, W., Li, Y., Wang, H., Huang, H., and Cui, X. (2012). Elongator complex is critical for cell cycle progression and leaf patterning in Arabidopsis. Plant J. *69*, 792–808.

Zhou, X., Hua, D., Chen, Z., Zhou, Z., and Gong, Z. (2009). Elongator mediates ABA responses, oxidative stress resistance and anthocyanin biosynthesis in Arabidopsis. Plant J. *60*, 79–90.

Zhou, F., Roy, B., and von Arnim, A.G. (2010). Translation reinitiation and development are compromised in similar ways by mutations in translation initiation factor eIF3h and the ribosomal protein RPL24. BMC Plant Biol. *10*, 193.

Cell Reports

Supplemental Information

Meta-regulation of *Arabidopsis* Auxin Responses Depends on tRNA Maturation

Johannes Leitner, Katarzyna Retzer, Nenad Malenica, Rasa Bartkeviciute, Doris Lucyshyn, Gunilla Jäger, Barbara Korbei, Anders Byström, and Christian Luschnig

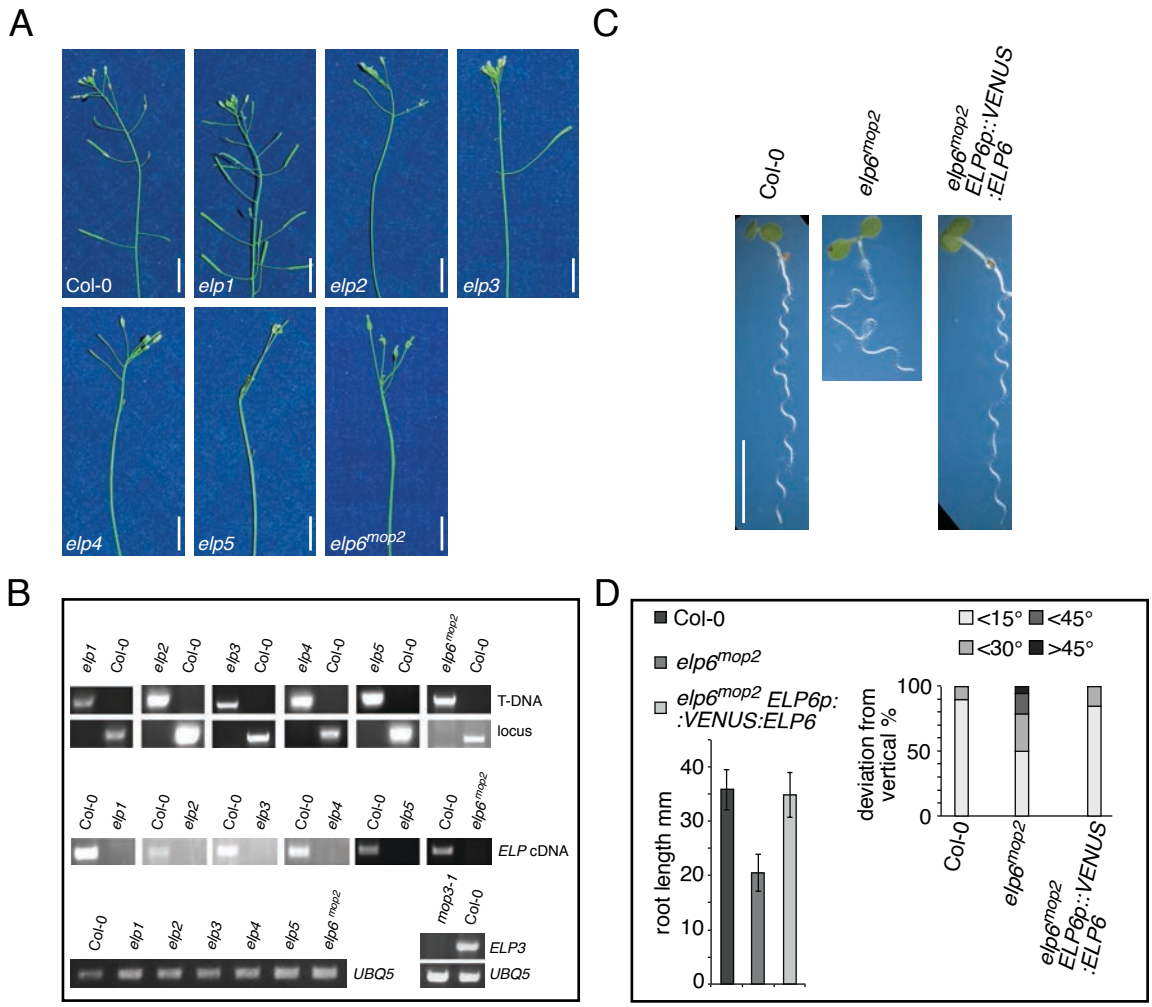

Figure S1, related to Figure 1: Identification and characterization of *elp/mop* loss-of-function mutants. **A)** Comparison of Col-0 and *elp* inflorescences at 35 DAG. Note aberrations in lateral organ positioning, characteristic for *Arabidopsis elp* mutants. **B)** Top panels: Genotyping of *elp* alleles performed with primers summarized in Table 1. Middle panels: RT-PCR analysis performed with *ELP* locus-specific primers for all 6 mutant loci. Col-0 cDNA was used as control. All cDNA samples gave a positive result with *UBQ5*-specific primers (bottom left). Bottom: RT-PCR performed with *mop3-1* and Col-0 cDNA. *Mop3-1* does not express a full-length *ELP3* transcript. *UBQ5* served as a control. **C)** 8-day-old Col-0, *elp6*^{mop2} and *elp6*^{mop2} *ELP6p::VENUS:ELP6* grown on vertically oriented agar plates. **D)** Left: Root length of Col-0, *elp6*^{mop2} and *elp6*^{mop2} *ELP6p::VENUS:ELP6* at 6 DAG. 30 seedlings were analyzed for each dataset. Standard deviations are indicated. Right: Directional root growth of Col-0, *elp6*^{mop2} and *elp6*^{mop2} *ELP6p::VENUS:ELP6* at 8 DAG. At least 40 seedlings were analyzed for each dataset. Size bars: A,C = 10 mm.

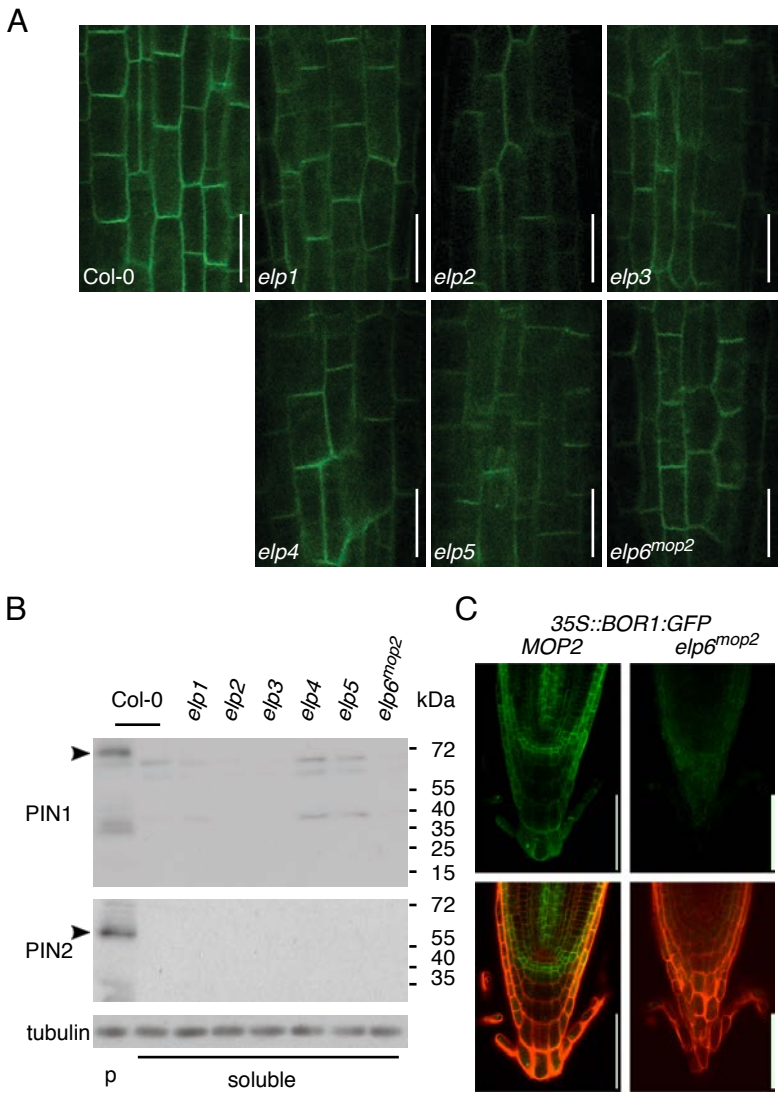

Figure S2, related to Figure 1: A) Distribution of *PIN1p::PIN1:GFP* signals (green) in wild type and *elp* mutant root meristem stele cells at 5 DAG. **B)** Western blot performed with soluble protein fractions derived from wild type and *elp* mutant protein extracts (6 DAG), probed with anti-PIN1 (top panel) and anti-PIN2 (middle panel). As a positive control, Col-0 membrane fraction protein extracts ("p") were used. Black arrowheads indicate position of PIN1- and PIN2-specific signals in the membrane fraction. Bottom panel displays signals obtained after probing with anti-tubulin. **C)** Expression of *35S::BOR1:GFP* (green) in *elp6*^{mop2}. *35S::BOR1:GFP* was crossed into *elp6*^{mop2} and resulting *MOP2* and *elp6*^{mop2} progeny, homozygous for the reporter protein was analyzed. Seedlings were stained with PI (red) to visualize cell boundaries. Size bars: A = 10 µm; C = 50 µm.

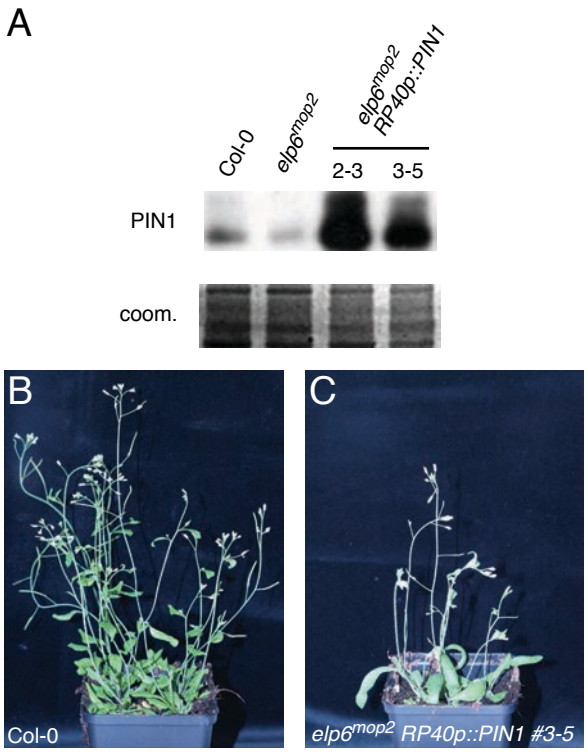

Figure S3, related to Figure 2: A) Determination of *PIN1* expression in *RP40p::PIN1* overexpression lines. Membrane proteins were extracted from 5-day-old seedlings, separated by SDS-PAGE and probed with anti-PIN1 antibody. Coomassie-staining (coom.) demonstrated comparable protein loading for all samples. **B,C)** Comparison of Col-0 (B) and *elp6*^{mop2} *RP40p::PIN1* (C) plants at the stage of flowering.

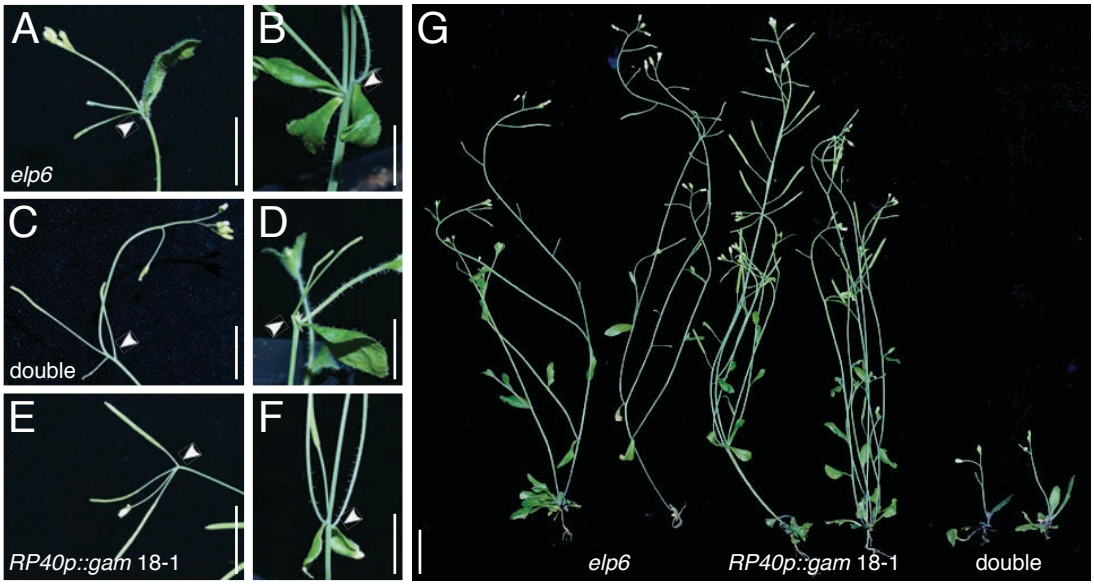

Figure S4, related to Figure 3: Comparison of *elp6*^{mop2}, *RP40p::gam* 18-1 and *elp6*^{mop2} *RP40p::gam* 18-1 ("double") at the stage of flowering. **A,B)** Details of *elp6*^{mop2} inflorescence (A) and inflorescence axes (B) at 30 DAG. **C,D)** Details of *elp6*^{mop2} *RP40p::gam* 18-1 ("double") inflorescence (C) and inflorescence axes (D) at 38 DAG. **E,F)** Details of *RP40p::gam* 18-1 inflorescence (E) and inflorescence axes (F) at 30 DAG. White arrowheads indicate aberrations in organ positioning (A-E). **G)** Comparison of *elp6*^{mop2}, *RP40p::gam* 18-1 and *elp6*^{mop2} *RP40p::gam* 18-1 ("double") plantlets at 30 DAG. Note the delay in growth of *elp6*^{mop2} *RP40p::gam* 18-1. Size bars: A-F = 10 mm; G = 20 mm.

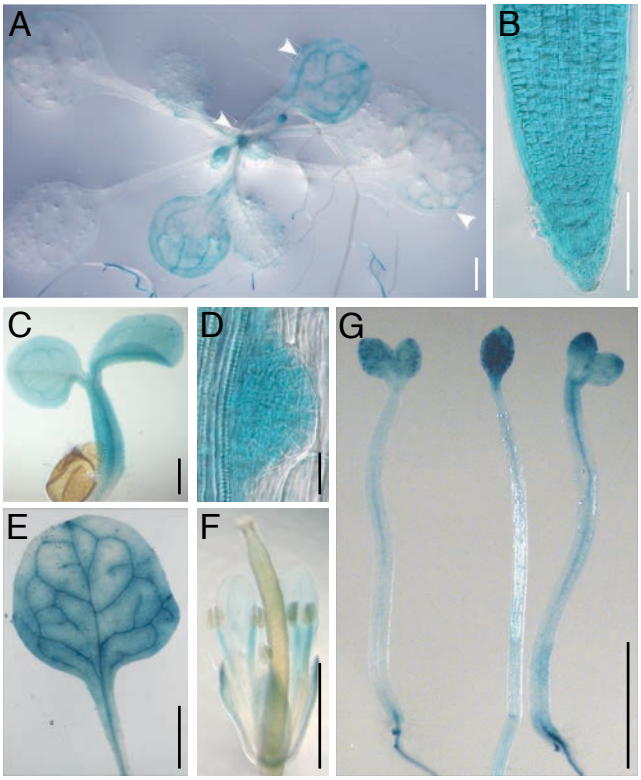

Figure S5, related to Figure 5: Expression of *AtRNLp::GUS* in Col-0. **A,B)** *AtRNLp::GUS* activity in a 12-day-old plantlet (A) and a primary root meristem (B). Arrowhead indicates pronounced GUS activity in vasculature and developing organs. **C)** Aerial portion of a seedling at 4 DAG. **D)** Later stage lateral root primordium. **E)** True Leaf. **F)** Flower. **G)** Etiolated hypocotyls: Size bars: A,E,G = 2 mm; B = 50 µm; C,F = 1 mm; D = 25 µm.

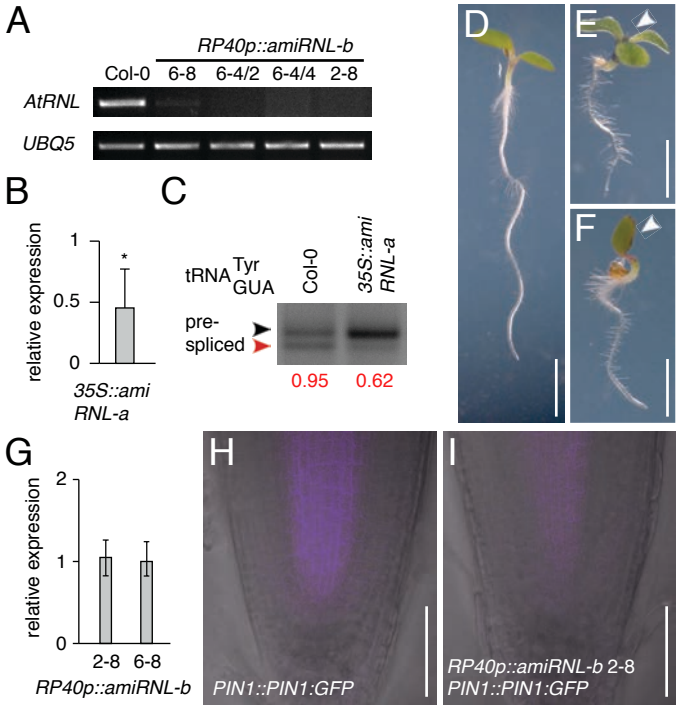

Figure S6, related to Figures 5 and 6: A) RT-PCR displaying *AtRNL* levels in 4 *RP40p::amiRNL-b* silencer lines. *UBQ5* was used for normalization. **B)** *AtRNL* transcript levels in a *35S::amiRNL-a* silencer line selected from 5 lines characterized by similar growth defects (Col0 = 1). Data from 3 biological repeats, each with 3 technical repeats are displayed. Standard deviations are shown (* = two-tailed t-test, $p < 0.05$). **C)** Quantification of $\mathrm{tRNA}^{\mathrm{Tyr}}_{\mathrm{GUA}}$ levels in Col-0 and *35S::amiRNL-a* by quantitative PCR. Upper band corresponds to non-spliced $\mathrm{tRNA}^{\mathrm{Tyr}}_{\mathrm{GUA}}$ precursor (black arrowhead); lower band corresponds to processed $\mathrm{tRNA}^{\mathrm{Tyr}}_{\mathrm{GUA}}$ (red arrowhead). Numbers below, display ratio between spliced and precursor band intensities. **D-F)** Comparison of Col-0 (D) and *35S::amiRNL-a* (E,F) seedlings at 4 DAG. *35S::amiRNL-a* develops shorter, slightly agravitropic roots and frequently shows an aberrant number of cotyledons (19/49; white arrowhead), which is not observed in wild type controls (0/45). **G)** Comparison of *PIN1* transcript levels in Col-0 and *RP40p::amiRNL-b* silencer lines 2-8 an 6-8 at 6 DAG (Col-0 = 1). Data from 3 biological repeats each with 3 technical repeats are displayed. Standard deviations are indicated. **H,I)** Expression of *PIN1p::PIN1:GFP* (purple) in Col-0 (H) and *RP40p::amiRNL-b* 2-8 (I) primary root meristems. Size bars: D-F = 5 mm; H,I = 50 μm.

Supplemental table: primers for expression analysis (Ex) and genotyping (Gt).

locus/primer	Application	5'-Sequence-3'
PIN2	Ex	GCTACTAAAGCGATGCAGAATC
PIN2	Ex	GAAATCGATCCACTCATTATCGTT
ELP1	Gt	TCTGATGATATAAGGAAAAAG
ELP1	Gt	GTATAGGCGCTCATTCCACT
ELP1	Ex	GGGGTTGGCTACTTTCCTGATT
ELP1	Ex	CTGCAAGCAATAATCGTCTCT
ELP2	Ex, Gt	CAGGATGCAACAGAGTCGTC
ELP2	Ex, Gt	TGTGTAACGGTAATGAGAAGTC
ELP3	Ex, Gt	GGCGGATCCATGGCGACGGCGGTAGTGA
ELP3	Ex, Gt	CATGCTTACTCTGTTAGTCCA
ELP4	Ex, Gt	CTGCACCAAACGTTCGTAGTAGTA
ELP4	Ex, Gt	TTGATAAAAACGTAGCACAG
ELP5	Ex, Gt	GTGGCGAAGAAGGCGAACTC
ELP5	Ex, Gt	AGCGCATTTGTGACCTTCTC
ELP6	Ex, Gt	CCGGATCCATGGATCGTTCTTTGAATCTCCTCGAT
ELP6	Ex, Gt	CCGGATCCTCAGCTTCTGCAACCAGGATAGAAATA
TUB9	Ex	ACTCGTTGGGAGGAGGAACT
TUB9	Ex	ACACCAGACATAGTAGCAGAAATCAAG
UBQ5	Ex	ACCCCTTGAGGTTGAATCATC
UBQ5	Ex	GTCCTTCTTTCTGGTAAACGT
LBa1	Gt	TGGTTCACGTAGTGGGCCATCG
LBb1	Gt	GCGTGGACCGCTTGCTGCAACT
RBa1	Gt	GCGGCTGAGTGGCTCTTCCAACGTT
RBb1	Gt	GTCGTTTCCCGCCTTCAGTTTAA
GKTd	Gt	ATATTGACCATCATACTCATTGC
PIN1	Ex	TACTCCGAGACCTTCCAACTACG
PIN1	Ex	TCCACCGCCACCACTTCC
tRNA-His	Ex	GTGGCTGTAGTTTAGTGGT
tRNA-His	Ex	TGTGGCTGGGATTCGAG
tRNA-Ser	Ex	GGACGTGCCGGAGTGGTTATCGGGCATGACT
tRNA-Ser	Ex	GAACGGCAGGATTCGAACCTGCGCGGGCAAA
tRNA-Gln	Ex	TTCTATGGTGTAGTGGTtAGCACTCTGGACTTT
tRNA-Gln	Ex	AGGTCCTACCGGGAGTCGAACCCAGGT
tRNA-Glu	Ex	GATGTCGTCCAGCGGTtAGGATATCT
tRNA-Glu	Ex	CTCCGTTACCGGGAATCGAACCC
AT5g60390	Ex	TGAGCACGCTCTTCTTGCTTTCA
AT5g60390	Ex	GGTGGTGGCATCCATCTTGTTACA
AtRNL	Ex	TTTATGTACGCCGGTCA
AtRNL	Ex	CGGTTACCAGTTCCATAG
γ-toxin	Ex	CAACCAAATGAAAGAAGAAGCTC
γ-toxin	Ex	CTCTTCTACCAAGACCTAATTC

Supplemental Experimental Procedures

Plant growth and lines

Plants were grown on 0.5x Murashige-Skoog or on plant nutrient agar medium (5 mM KNO_3, 2 mM $MgSO_4$, 2 mM $Ca(NO_3)_2$, 250 mM KPO_4, 70 μM H_3BO_3, 14 μM $MnCl_2$, 500nM $CuSO_4$, 1 μM $ZnSO_4$, 200 nM Na_2MoO_4, 10 μM NaCl, 10 nM $CoCl_2$, 50 μM $FeSO_4$; pH adjusted to 5.7; supplemented with 1% (w/v) agar and 1% (w/v) sucrose (Haughn and Somerville, 1986); in a 16 hrs. light/8 hrs. dark regime at 22°C, if not indicated otherwise. *DR5rev::GFP*, *PIN1p::PIN1:GFP*, *35S::YFP:ELP3*, *35S::YFP:GCN5*, *35S::BOR1:GFP* reporter lines as well as *mop2-1* and *mop3-1* have been described elsewhere (Benkova et al., 2003; Earley et al., 2007; Malenica et al., 2007; Takano et al., 2005). For analysis of *AtRNL*, T-DNA insertion lines SALK_059581, SAIL_693_G06 and GK-258C06 were genotyped and tested for effects on transcription by using oligonucleotides 5'- AGCTCGCTTAGCTCAGATGA-3', 5'- GGCTCTGATCTGAGCATGAC-3', 5' CGGCTGTCTCACAGATAGGT-3', 5'-CCTAACTCGGTAACAGCAGTC-3', 5'- GCAAACCCAACAATGAGATC-3', 5'-GATATCTCAATGAATGCAG-3', 5'- GGGCTTACTGTGGCCCAATAG-3' and 5'-AACGACATCAACACGTGGC-3'. No differences in gene expression were observed in the SALK and SAIL lines, whereas we failed to identify a T-DNA insertion in the GABI line. We therefore decided to initiate an amiRNA silencing approach.

For determination of growth, seedlings and adult plants were analyzed at indicated time points. Root length, lateral root growth and root gravitropism were assessed manually on vertically grown seedlings. For determination of cotyledon vasculature seedlings were cleared in 70% (v/v) EtOH and viewed on a binocular. Phenotypes of flowering plants were determined on soil-grown seedlings incubated in a growth chamber at a 16 hrs. light/8 hrs. dark regime at 22°C. For analysis of *RP40p::PIN1* expression in *elp6*^{mop2} and wild type, we compared isogenic lines

obtained by crossing of and identification of double homozygote lines in resulting progeny generations For root growth assays, we used line *RP40p::PIN1* #2-3. Similarly, for analysis of *RP40p::gam* in *elp6*^{mop2} we obtained isogenic lines by crossing *RP40p::gam* and *elp6*^{mop2} parental lines. Effects of hormones and growth regulators were assessed by adding appropriate amounts of the compounds, dissolved as 1000x stocks in either EtOH or DMSO. Solvent only was added to the control medium.

Generation of constructs

For generation of *RP40p::PIN1* the *PIN1* cDNA was cloned into RP40p-pApA, a derivative of pPZP221 (Butt et al., 2014). For generation of *RP40p::gam* we amplified γ-toxin lacking its signal peptide by using 5'-GGCCCGGGATGAAGATATATCATATATTTAGTG-3' and 5'-GGCCCGGGTTAGTCGACTACACATTTTCCATTCTGTAGATTA-3' according to Lu and colleagues (Lu et al., 2005). The confirmed clone was then introduced into RP40p-pApA.

For *ELP6::VENUS:ELP6* the *ELP6* cDNA was amplified using oligonucleotides 5'-CCGGATCCATGGATCGTTCTTTGAATCTCCTCGAT-3' and 5'-CCGGATCCTCAGCTTCTGCAACCAGGATAGAAATA-3', and cloned into pApA–pPZP221 (Leitner et al., 2012), 3' of an *ELP6* promoter fragment amplified with oligonucleotides 5'-CCGAATTCAAATATATAAACAAGTTTTTGGAA-3' and 5'-CCGAATTCGGAGAAATTTGGACGGAGAAGAAGA-3'. A VENUS tag (Nagai et al., 2002) was then introduced in frame immediately upstream of the *ELP6* Start-ATG.

For generation of silencer constructs, we used oligonucleotides 5'-GATATAGACTCAAATGGAACCTCTCTCTCTTTTGTATTCC-3', 5'-GAGAGGTTCCATTTGAGTCTATATCAAAGAGAATCAATGA-3', 5'-

GAGAAGTTCCATTTGTGTCTATTTCACAGGTCGTGATATG-3' and 5'-GAAATAGACACAAATGGAACTTCTCTACATATATATTCCT-3' to generate amiRNL-a directed against nucleotides 2969-2987 of the *AtRNL* cDNA. For amiRNL-b directed against 1203-1218 of the *AtRNL* cDNA we employed oligonucleotides 5'-GATACTGCTCACGATACGACCAATCTCTCTTTTGTATTCC-3', 5'-GATTGGTCGTATCGTGAGCAGTATCAAAGAGAATCAATGA-3', 5'-GATTAGTCGTATCGTCAGCAGTTTCACAGGTCGTGATATG-3' and 5'-GAAACTGCTGACGATACGACTAATCTACATATATATTCCT-3'. Resulting constructs were expressed under control of either the 35S-promoter (amiRNL-a), or the *RP40*-promoter (amiRNL-b). For generation of *AtRNLp::GUS* we used oligonucleotides 5'-GCTGTATATCTCCTCAATTGCTGATT-3' and 5'-CTTCGGTTTTACTTGCCACTTCTGC-3' to amplify a 2.2 kb *AtRNL* promoter fragment for expression of the GUS reporter gene in pPZP-GUS (Diener et al., 2000).

Expression analysis

For analysis of tRNA modifications in *elp* mutants, total RNA was isolated from 100 g Col-0, *elp3* and *elp6*^{mop2} seedlings, grown in liquid medium (23°C, 16 light, 6-days-old). Plant material was ground with mortar and pestle and ice-cold 0.9 % NaCl was added (2 ml/g), vortexed immediately and the same amount of phenol was added afterwards. Samples were homogenized on an orbital shaker for 30 min., followed by centrifugation at 10.000 x g for 30 min. The aqueous phase was re-extracted and precipitated with 0.7 vol. of isopropanol o/n at -20°C. After washing and drying, RNA pellets were dissolved in 2 ml of 2 M LiCl/0.05 M NH_4OAc and vortexed vigorously for 10 min, followed by o/n precipitation of mRNAs and ribosomal RNAs on ice. After centrifugation at 4°C for 30 min at 10.000 x g, supernatant fractions were precipitated with 2.5 vol of ice-cold EtOH o/n at -20°C. Small RNAs

were pelleted by centrifugation at 4°C for 30 min at 10.000 x g and washed in 70 % EtOH. Pellets were air-dried and resuspended in 100 µl RNase-free water. RNA integrity was analyzed on 2 % agarose gels and concentration was determined spectrophotometrically.

For analysis of $tRNA^{Tyr}$ splicing, cDNA from small RNA pools pretreated with RNAse-free DNAse-I (Roche, Vienna, Austria) was generated by using primer 5'-TCCGACCGGATTCGAACCAGTGA-3' to enrich for $tRNA^{Tyr}$ transcripts. cDNA samples were then used for PCR with primers 5'-CGGCTGTCTCACAGATAGGT-3' and 5'-CCTAACTCGGTAACAGCAGTC-3, specifically amplifying spliced and unprocessed $tRNA^{Tyr}$ followed by separation by gel electrophoresis. Relative signal intensities were determined by Image-J software.

For semi-quantitative RT-PCR we generated cDNA from mRNA samples according to Sieberer and colleagues (Sieberer et al., 2003). For qPCR we generated cDNA from total RNA samples by using the QuickPick™ total RNA isolation kit from BioNobile (Pargas, Finland). DNAseI (Roche, Vienna, Austria) treatment was performed after sample elution followed by reverse transcription with M-MuLV H plus Reverse Transcriptase (peqLab, Erlangen, Germany) in presence of either oligo-dT for generation of mRNA-derived cDNAs, or random hexameric primers for total RNA conversion. PCR was performed on a CFX96 Real Time System (Biorad, Hercules, CA, USA). Data were analyzed with CFX Manager Software (Bio Rad, version 2.1), Cq values were determined by single threshold methods, and combined data derived from biological replicates are presented (Livak and Schmittgen, 2001). For normalization, we used locus At5g60390 (*EF-1a*) for mRNA expression analysis (Czechowski et al., 2005). For determination of $\mathrm{tRNA}^{\mathrm{Gln}}_{\mathrm{UUG}}$ and $\mathrm{tRNA}^{\mathrm{Glu}}_{\mathrm{UUC}}$ abundance we normalized against levels of $\mathrm{tRNA}^{\mathrm{His}}_{\mathrm{GUG}}$ and $\mathrm{tRNA}^{\mathrm{Ser}}_{\mathrm{AGA}}$, which due to the absence of wobble uridines should not represent preferred

substrates for γ-toxin. Relative tRNA abundance in *RP40p::gam* lines was normalized to tRNA abundance obtained in wild type controls. Oligonucleotides used for expression analyses are summarized in the Supplemental Table.

Membrane protein extraction has been performed according to Leitner et al., (2012). In brief, root material was homogenized and resuspended in extraction buffer, as described previously (Abas and Luschnig, 2010). Samples were cleared by centrifugation (2,100 × g for 2 min). The supernatant was saved and the pellet was re-extracted. Samples were cleared by centrifugation, and combined supernatants were centrifuged (14,000 × g for 2 hours) to yield total membrane pellets. For Western blot analysis, membrane pellets or proteins precipitated from the supernatant were resuspended in sample buffer [0.5% (wt/vol) CHAPS, 3% (wt/vol) SDS, 30% (vol/vol) glycerol, 60 mM dithioerythritol, 50 mM Tris (pH 6.8), 1 mM PMSF, and 0.5x Roche Complete Mini Protease Inhibitor Mixture Tablets; (Abas and Luschnig, 2010)]. Proteins were separated by SDS/urea PAGE, transferred to nitrocellulose membranes, and probed with affinity-purified rabbit anti-PIN1 and anti-PIN2 (Abas and Luschnig, 2010), followed by HRP-conjugated goat-anti-rabbit IgG (1:20,000; Pierce). Mouse-anti-Tubulin (Sigma) was used for normalization, and detected after probing with HRP-conjugated rabbit-anti-mouse IgG (1: 10,000; Jackson).

For visualization of FP-tagged reporter lines, we used Leica SP2 and SP5 Confocal Laser Scanning Microscopes (CLSM). Seedlings were viewed either alive after brief staining in propidium iodide (100 µg/ml) to visualize cell boundaries, or after fixation in 3.7 % (v/v) formaldehyde in Microtubule Stabilization Buffer (MTSB; 50 mM PIPES, 5 mM EGTA, 5 mM $MgSO_4$) for 15 minutes. After 3 washes in MTSB seedlings were mounted in MTSB containing 4,6,Diamidine-2-phenylindole

dihydrochloride (DAPI, 0.5 ng/ml) and viewed under the CLSM. For imaging, we used the following excitation conditions: 488 nm (GFP), 514 nm (VENUS, YFP), 405 nm (DAPI), 561 nm (propidium iodide).

HPLC analysis of tRNAs

Purified tRNA was digested with Nuclease P1 for 16 h at 37°C and then treated with bacterial alkaline phosphatase for 2 h at 37°C. The hydrolysate was analyzed by high-pressure liquid chromatography with a Develosil C-30 reversed-phase column as described (Gehrke et al., 1982; Gehrke and Kuo, 1990).

Supplemental References

Abas, L., and Luschnig, C. (2010). Maximum yields of microsomal-type membranes from small amounts of plant material without requiring ultracentrifugation. Anal Biochem *401*, 217-227.

Benkova, E., Michniewicz, M., Sauer, M., Teichmann, T., Seifertova, D., Jurgens, G., and Friml, J. (2003). Local, efflux-dependent auxin gradients as a common module for plant organ formation. Cell *115*, 591-602.

Butt, H., Graner, S., and Luschnig, C. (2014). Expression analysis of Arabidopsis XH/XS-domain proteins indicates overlapping and distinct functions for members of this gene family. J Exp Bot *65*, 1217-1227.

Czechowski, T., Stitt, M., Altmann, T., Udvardi, M.K., and Scheible, W.R. (2005). Genome-wide identification and testing of superior reference genes for transcript normalization in Arabidopsis. Plant Physiol *139*, 5-17.

Diener, A.C., Li, H., Zhou, W., Whoriskey, W.J., Nes, W.D., and Fink, G.R. (2000). Sterol methyltransferase 1 controls the level of cholesterol in plants. Plant Cell *12*, 853-870.

Earley, K.W., Shook, M.S., Brower-Toland, B., Hicks, L., and Pikaard, C.S. (2007). In vitro specificities of Arabidopsis co-activator histone acetyltransferases: implications for histone hyperacetylation in gene activation. Plant J *52*, 615-626.

Gehrke, C.W., Kuo, K.C., McCune, R.A., Gerhardt, K.O., and Agris, P.F. (1982). Quantitative enzymatic hydrolysis of tRNAs: reversed-phase high-performance liquid chromatography of tRNA nucleosides. J Chromatogr *230*, 297-308.

Gehrke, C.W., and Kuo, K.C.T. (1990). Chromatography and Modification of Nucleosides (Amsterdam, Elsevier).

Haughn, G.W., and Somerville, C. (1986). Sulfonylurea-resistant mutants of Arabidopsis
thaliana. Mol Gen Genet *204*, 430-434.

Leitner, J., Petrasek, J., Tomanov, K., Retzer, K., Parezova, M., Korbei, B., Bachmair, A., Zazimalova, E., and Luschnig, C. (2012). Lysine63-linked ubiquitylation of PIN2 auxin carrier protein governs hormonally controlled adaptation of Arabidopsis root growth. Proc Natl Acad Sci U S A *109*, 8322-8327.

Livak, K.J., and Schmittgen, T.D. (2001). Analysis of relative gene expression data using real-time quantitative PCR and the 2(-Delta Delta C(T)) Method. Methods *25*, 402-408.

Lu, J., Huang, B., Esberg, A., Johansson, M.J., and Bystrom, A.S. (2005). The Kluyveromyces lactis gamma-toxin targets tRNA anticodons. Rna *11*, 1648-1654.

Malenica, N., Abas, L., Benjamins, R., Kitakura, S., Sigmund, H.F., Jun, K.S., Hauser, M.T., Friml, J., and Luschnig, C. (2007). MODULATOR OF PIN genes control steady-state levels of Arabidopsis PIN proteins. Plant J *51*, 537-550.

Nagai, T., Ibata, K., Park, E.S., Kubota, M., Mikoshiba, K., and Miyawaki, A. (2002). A variant of yellow fluorescent protein with fast and efficient maturation for cell-biological applications. Nat Biotechnol *20*, 87-90.

Sieberer, T., Hauser, M.T., Seifert, G.J., and Luschnig, C. (2003). PROPORZ1, a putative Arabidopsis transcriptional adaptor protein, mediates auxin and cytokinin signals in the control of cell proliferation. Curr Biol *13*, 837-842.

Takano, J., Miwa, K., Yuan, L., von Wiren, N., and Fujiwara, T. (2005). Endocytosis and degradation of BOR1, a boron transporter of Arabidopsis thaliana, regulated by boron availability. Proc Natl Acad Sci U S A *102*, 12276-12281.